MEE09:58

CHANNEL ESTIMATION FOR LTE DOWNLINK

Asad Mehmood

Waqas Aslam Cheema

This thesis is presented as part of Degree of Master of Science in Electrical Engineering

Blekinge Institute of Technology

September 2009

Blekinge Institute of Technology
School of Engineering
Department of Signal Processing
Supervisor Prof. Abbas Mohammed
Examiner Prof. Abbas Mohammed

Abstract

3GPP LTE is the evolution of the UMTS in response to ever-increasing demands for high quality multimedia services according to users' expectations. Since downlink is always an important factor in coverage and capacity aspects, special attention has been given in selecting technologies for LTE downlink. Novel technologies such as orthogonal frequency division multiplexing (OFDM) and multiple input, multiple output (MIMO), can enhance the performance of the current wireless communication systems. The high data rates and the high capacity can be attained by using the advantages of the two technologies. These technologies have been selected for LTE downlink.

Pilot-assisted channel estimation is a method in which known signals, called pilots, are transmitted along with data to obtain channel knowledge for proper decoding of received signals. This thesis aims at channel estimation for LTE downlink. Channel estimation algorithms such as Least Squares (LS), Minimum Mean Square Error (MMSE) haven been evaluated for different channel models in LTE downlink. Performance of these algorithms has been measured in terms of Bit Error Rate (BER) and Symbol Error Rate (SER).

ACKNOWLEGEMENT

All praises and thanks to Almighty ALLAH, the most beneficent and the most merciful, who gave us the all abilities and helped us to complete this research work.

We would like to express our sincere gratitude to our supervisor Prof. Abbas Mohammed for his support and guidance during the course of this work. His encouragement and guidance has always been a source of motivation for us to explore various aspects of the topic. Discussions with him have always been instructive and insightful and helped us to identify our ideas.

Finally, we are very grateful to our parents, brother and sisters for their sacrifices, unremitting motivation and everlasting love and their continuous support during our stay in BTH.

Table of Contents

List of Figures

List of Tables

Chapter 1 Introduction

1.1) Introduction

During the last decade along with continued expansion of networks and communications technologies and the globalization of 3rd Generation of Mobile Communication Systems, the support for voice and data services have encountered a greater development compared to 2nd Generation Systems. At the same time the requirements for high quality wireless communications with higher data rates increased owing to users demands. On the other hand, the conflict of limited bandwidth resources and rapidly growing numbers of users becomes exceptional, so the spectrum efficiency of system should be improved by adopting some advanced technologies. It has been demonstrated in both theory and practice that some novel technologies such as orthogonal frequency division multiplexing (OFDM) and multiple input, multiple output (MIMO) systems, can enhance the performance of the current wireless communication systems. The high data rates and the high capacity can be attained by using the advantages of the two technologies. From a standardization perspective 3G era is now well-advanced. While enhancements continue to be made to leverage the maximum performance from currently deployed systems, there is a bound to the level to which further improvements will be effective. If the only purpose were to deliver superior performance, then this in itself would be relatively easy to accomplish. The added complexity is that such superior performance must be delivered through systems which are cheaper from installation and maintenance prospect. Users have experienced an incredible reduction in telecommunications charges and they now anticipate receiving higher quality communication services at low

cost. Therefore, in deciding the subsequent standardization step, there must be a dual approach; in search of substantial performance enhancement but at reduced cost. Long Term Evolution (LTE) is that next step and will be the basis on which future mobile telecommunications systems will be built. LTE is the first cellular communication system optimized from the outset to support packet-switched data services, within which packetized voice communications are just one part.

The 3rd Generation Partnership Project (3GPP) started work on Long Term Evolution in 2004 with the description of targets illustrated in [1]. The specifications associated to LTE are formally identified as the evolved UMTS terrestrial radio access network (E-UTRAN) and the evolved UMTS terrestrial radio access (E-UTRA). These are collectively referred to by the project name LTE. In December 2008, release 8 of LTE has been approved by 3GPP which will allow network operators to appreciate their deployment plans in implementing this technology. A few motivating factors can be identified in advancing LTE development; enhancements in wire line capability, the requirement for added wireless capacity, the need for provision of wireless data services at lower costs and the competition to the existing wireless technologies. In addition to the continued advancement in wire line technologies, a similar development is required for technologies to work fluently with defined specifications in the wireless domain. 3GPP technologies must match and go beyond the competition with other wireless technologies which guarantee high data capabilities – including IEEE 802.16. To take maximum advantage of available spectrum, large capacity is an essential requirement. LTE is required to provide superior performance compared to High Speed Packet Access (HSPA) technology according to 3GPP specifications. The 3GPP LTE release 8 specification defines the basic functionality of a new, high-performance air interface providing high user data rates in combination with low latency based on MIMO, OFDMA (orthogonal frequency division multiple access), and an optimized system architecture

evolution (SAE) as main enablers. The LTE solution provides spectrum flexibility with scalable transmission bandwidth between 1.4 MHz and 20 MHz depending on the available spectrum for flexible radio planning. The 20 MHz bandwidth can provide up to 150 Mbps downlink user data rate and 75 Mbps uplink peak data rate with 2 × 2 MIMO, and 300 Mbps with 4 × 4 MIMO. A summary of release 8 can be found in [2].

1.2) Objectives

In deciding the technologies to comprise in LTE, one of the key concerns is the trade-off between cost of implementation and practical advantage. Fundamental to this assessment, therefore, has been an enhanced understanding different scenarios of the radio propagation environment in which LTE will be deployed and used.

The effect of radio propagation conditions on the transmitted information must be estimated in order to recover the transmitted information accurately. Therefore channel estimation is a vital part in the receiver designs of LTE. In this thesis work, a detailed study of standard channel models based on ITU and 3GPP recommendations for LTE has been done. The main focus of the work is to investigate and evaluate the channel estimation techniques such as Minimum Mean Square Channel Estimation, Least Square Channel Estimation and Down Sampled Channel Impulse Response Least Square Estimation for LTE down link. Therefore a link level simulator based on LTE physical layer specifications [3] has been presented. This simulator emulates channel estimation algorithms for standard channel models defined for LTE, using MIMO-OFDM and multi-level modulation schemes in LTE down link between the eNodeB and the user equipment (UE). The performance of the link level simulator is measured in terms

of bit error rate (BER) and symbol error rate (SER) averaged over all channel realizations of different propagation environments.

1.3) Out Line of the Master Thesis

This thesis work is divided into seven chapters:

- Chapter 1 about the introduction of LTE describing the background, the role of the technology in the present mobile communication systems and the motivation of this master thesis.

- Chapters 2 gives details about LTE Air Interface features describing LTE down link fame structure and the transmission techniques used in LTE.

- In Chapter 3, block diagram of system model used in the simulation of LTE down link physical layer is presented.

- Chapter 4 gives details of radio propagation models for LTE. The chapter describes the basics of multipath channel modeling following standard channel models for UMTS and LTE including SISO and MIMO channel models based on ITU recommendations.

- Chapter 5 evaluates the channel estimation algorithms including Minimum Mean Square Channel Estimation, Least Square Channel Estimation and Down Sampled Channel Impulse Response Least Square Estimation using channel models described in Chapter 4 for Single Input Single Output (SISO) systems.

- In chapter 6 the channel estimation algorithms are evaluated for MIMO systems.

- Chapter 7 goes over the main points of this thesis work with concluding remarks and proposes future work that can be done with the simulator used in this thesis in order to continue investigation within LTE Air Interface.

Chapter 2 Overview of LTE Physical Layer

2.1) Introduction

As compared to previous used cellular technologies like UMTS (universal mobile technology systems) or high speed down-link packet access (HSDPA), the Physical Layer of LTE is designed to deliver high data rate, low latency, packet-optimized radio access technology and improved radio interface capabilities. Wireless broadband internet access and advanced data services will be provided by this technology.

LTE physical Layer will provide peak data rate in uplink up to 50 Mb/s and in downlink up to 100 Mb/s with a scalable transmission bandwidth ranging from 1.25 to 20 MHz to accommodate the users with different capacities. For the fulfillments of the above requirements changes should be made in the physical layer (e.g., new coding and modulation schemes and advanced radio access technology). In order to improve the spectral efficiency in downlink direction, Orthogonal Frequency Division Multiple Access (OFDMA), together with multiple antenna techniques is exploited. In addition, to have a substantial increase in spectral efficiency the link adaption and frequency-domain scheduling are exercised to exploit the channel variation in time/frequency domain. LTE air interface exploits both time division duplex (TDD) and frequency division duplex (FDD) modes to support unpaired and paired spectra [4,5]. The transmission scheme used by LTE for uplink transmission is SC-FDMA (Signal Carries Frequency Division Multiple Access). For more detailed description of LTE physical layer covering uplink and downlink in see [6,7].

2.2) Objectives of LTE Physical Layer

The objectives of LTE physical layer are; the significantly increased peak data rates up to 100Mb/s in downlink and 50 Mb/s in uplink within a 20 MHz spectrum leading to spectrum efficiency of 5Mb/s, increased cell edge bit rates maintain site locations as in WCDMA, reduced user and control plane latency to less than 10 ms and less than 100 ms, respectively [8], to provide interactive real-time services such as high quality video/audio conferencing and multiplayer gaming, mobility is supported for up to 350 km/h or even up to 500 km/h and reduced operation cost. It also provides a scalable bandwidth 1.25/2.5/5/10/20MHz in order to allow flexible technology to coexist with other standards, 2 to 4 times improved spectrum efficiency the one in Release 6 HSPA to permit operators to accommodate increased number of customers within their existing and future spectrum allocation with a reduced cost of delivery per bit and acceptable system and terminal complexity, cost and power consumption and the system should be optimized for low mobile speed but also support high mobile speed as well.

2.3) Frame Structure

Two types of radio frame structures are designed for LTE: Type-1 frame structure is applicable to Frequency Division Duplex (FDD) and type-2 frame structure is related to Time Division Duplex (TDD). LTE frame structures are given in details in [3].

2.3.1) Type-1 Frame Structure

Type 1 frame structure is designed for frequency division duplex and is valid for both half duplex and full duplex FDD modes. Type 1 radio frame has a duration 10ms and consists of equally sized 20 slots each of 0.5ms. A sub-frame comprises two slots, thus one radio frame has 10 sub-frames as illustrated in figure 2.1. In

FDD mode, half of the sub-frames are available for downlink and the other half are available for uplink transmission in each 10ms interval, where downlink and uplink transmission are separated in the frequency domain [2].

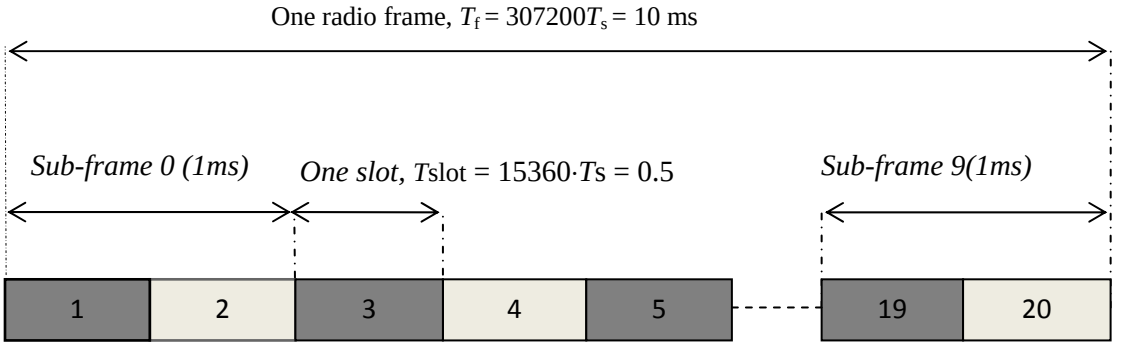

Figure 2.1: Frame structure of type 1(Ts is expressing basic time unit corresponding to 30.72MHz)

2.3.2) Type-2 Frame Structure

Type 2 frame structure is relevant for TDD; the radio frame is composed of two identical half-frames each one having duration of 5ms. Each half-frame is further divided into 5 sub-frames having duration of 1ms as demonstrated in figure 2.2. Two slots of length 0.5ms constitute a sub-frame which is not special sub-frame. The special type of sub-frames is composed of three fields Downlink Pilot Timeslot (DwPTS), GP (Guard Period) and Uplink Pilot Timeslot (UpPTS). Seven uplink-downlink configurations are supported with both types (10ms and 5ms) of downlink-to-uplink switch-point periodicity. In 5m downlink-to-uplink switch-point periodicity, special type of sub-frames are used in both half-frames but it is not the case in 10ms downlink-to-uplink switch-point periodicity, special frame are used only in first half-frame. For downlink transmission sub-frames 0, 5 and DwPTS are always reserved. UpPTS and the sub-frame next to the special sub-frame are always reserved for uplink communication [3]. The supporting downlink-uplink configuration is shown in table 2.1 where U and D donate the sub-frames reserved

for uplink and downlink, respectively, and S denotes the reserved sub-frames as illustrated in table 2.1.

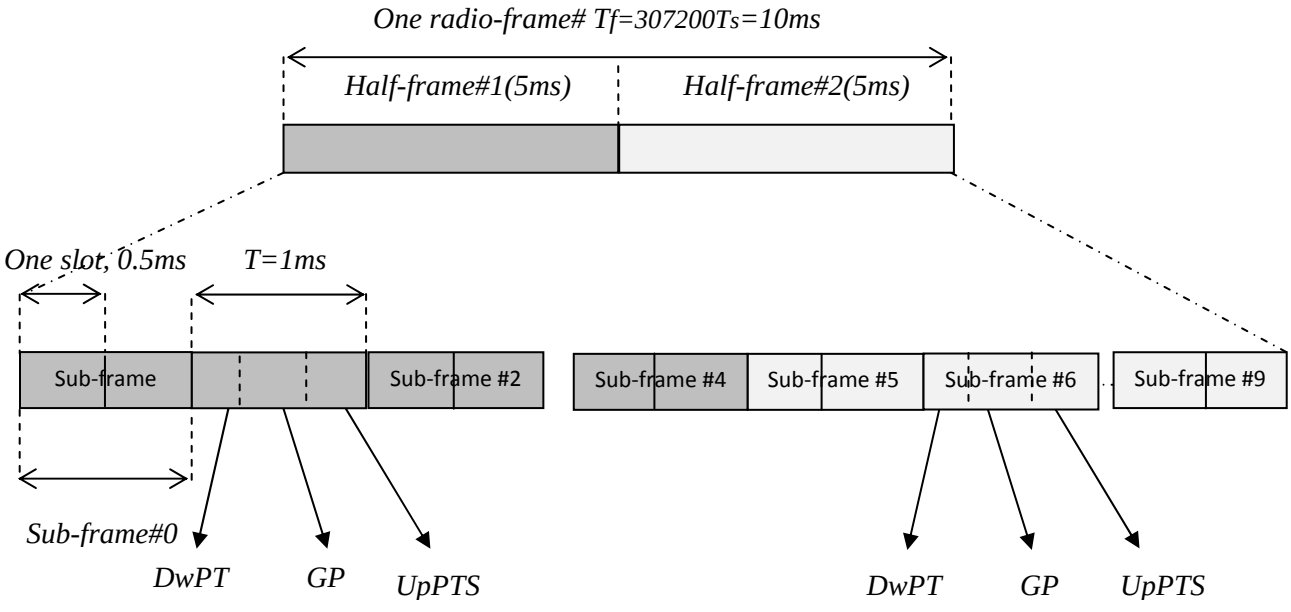

Figure 2.2: Frame structure type-2 (for 5 ms switch-point periodicity)

Uplink-Downlink configuration	Downlink-to-uplink Switch-point periodicity	Sub-frame Numbers									
		0	1	2	3	4	5	6	7	8	9
0	5ms	D	S	U	U	U	D	S	U	U	U
1	5ms	D	S	U	U	D	D	S	U	U	D
2	5ms	D	S	U	D	D	D	S	U	D	D
3	10ms	D	S	U	U	U	D	D	D	D	D
4	10ms	D	S	U	U	D	D	D	D	D	D
5	10ms	D	S	U	D	D	D	D	D	D	D
6	5ms	D	S	U	U	U	D	S	U	U	D

Table 2.1 Uplink-Downlink configurations for LTE TDD [3]

2.4) Physical Resource and Slot structure

In each available slot the transmitted signal can be seen as a time-frequency recourse gird, where each recourse element (RE) corresponds to one OFDM sub-carrier during OFDM symbol interval. The number of sub-carriers is being determined by the transmission bandwidth. For normal cyclic prefix (CP) each slot contains seven OFDM symbols and in case of extended cyclic prefix, 6 OFDM symbols are slotted-in in each time slot. The different lengths of CP are mention in Table 2.1. In this work we have used two types of CP lengths, short and extended, with Type 1 frame structure.

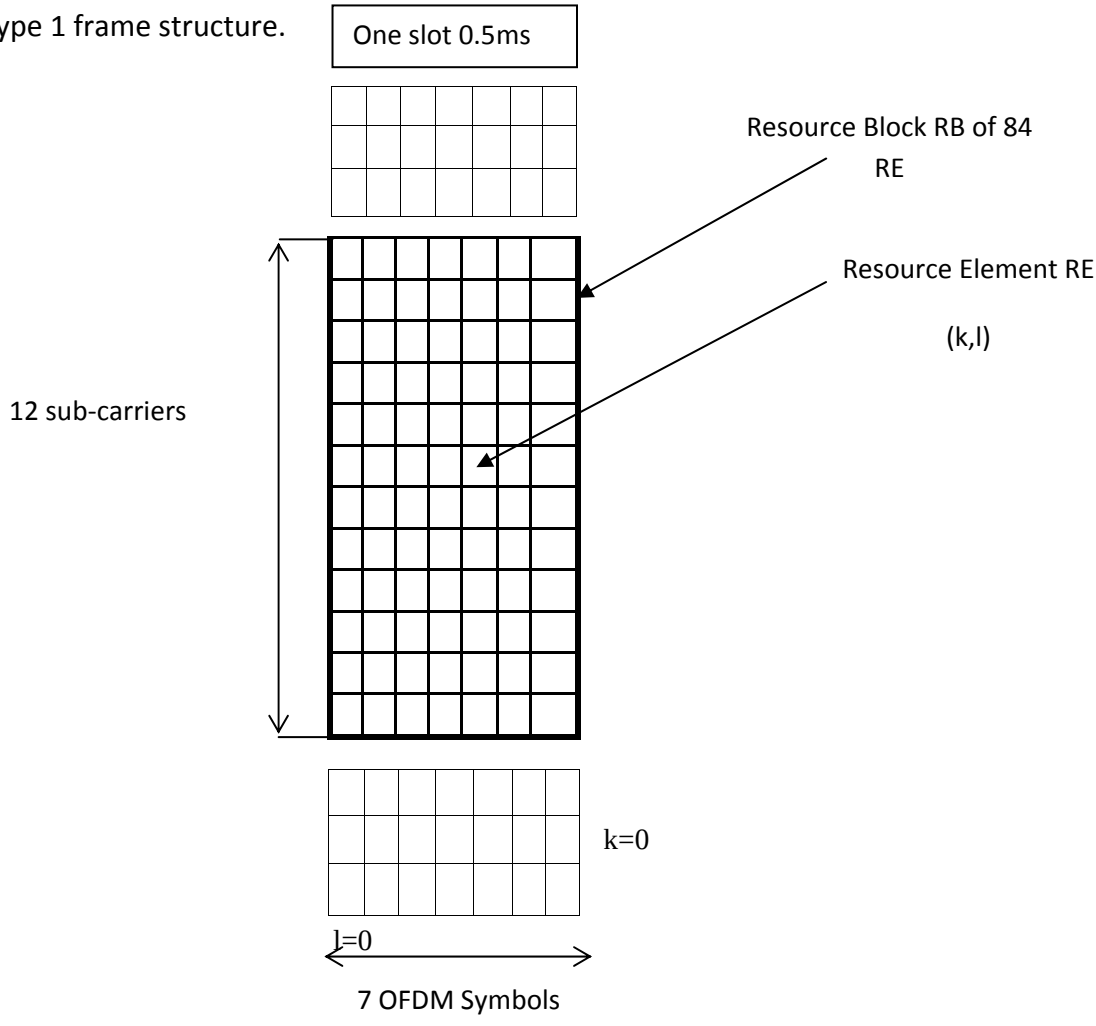

Figure 2.3: Downlink Resource grid [3]

In LTE downlink a constant sub-carriers spacing of 15 kHz is utilized. In frequency domain, 12 sub-carriers are grouped together to form a Resource Block (RB) occupying total 180 kHz in one slot duration as illustrated in figure 2.3. In case of short CP, length a resource block contains 84 resource elements (RE) and for long CP the number of RE is 74. For multiple antenna schemes, there will be one resource gird per antenna [3,9]. For all available bandwidths, the size of resource blocks is the same.

2.5) LTE Downlink Reference Signals Structure

In order to carry out coherent demodulation in LTE down link, channel estimation is needed at the receiver end. In case of OFDM transmission known reference symbols are added into time-frequency grid for channel estimation. These signals are called LTE Downlink Reference signals [10]. For time domain, reference symbols are slotted-in in the first and the third last elements of resource grid, where as reference signals are inserted over every six sub-carriers in frequency domain. For an accurate channel estimation over entire gird and reducing noise in channel estimates, a two-dimensional time-frequency interpolation/averaging is required over multiple reference symbols. One reference signal is transmitted from each antenna to estimate the channel quality corresponding to each path when a multiple antenna scheme is applied. In this case, reference signals are mapped on different sub-carries of resource grid for different antennas to refrain from interference. Resource elements used to transmit reference signals from antenna-1 are not reused on antenna-2 for data transmission; these places are filled with zeros. Allocation of these reference symbols is shown in figure 2.4 [4,10].

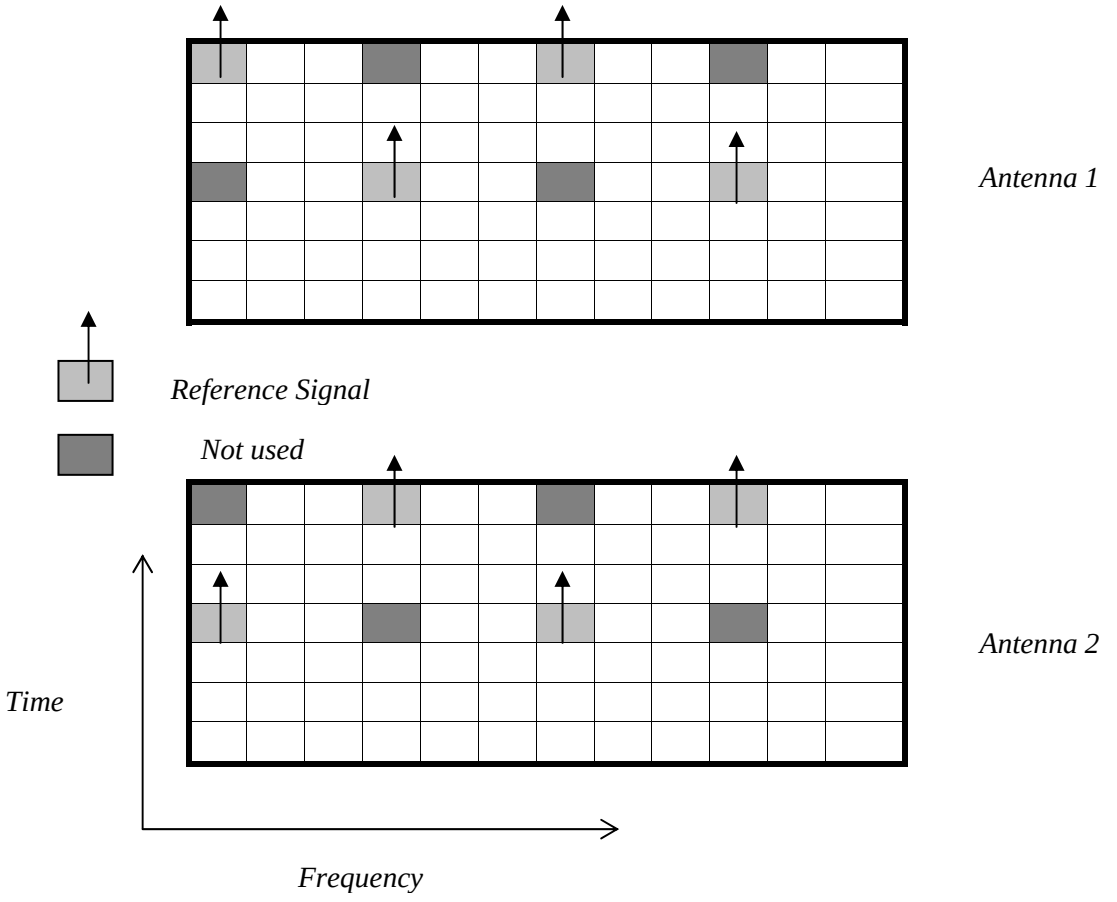

Figure 2.4: Allocation of Reference Symbols for two antenna transmissions

2.6) LTE Downlink Parameters

As mentioned in above section that LTE ropes scalable bandwidth, so the number of sub-carries also changes while keeping sub-carriers spacing up to 15 kHz. Depending on the delay spread, two CP lengths (short and extended) are allowed. It also aims at supporting different scenarios, indoor, urban, suburban and rural for both kinds of mobility conditions (Low and High) of mobile terminal ranging from 350Km/h to 500km/h. While using FDD configuration same frame structure

and parameters are used in uplink and downlink. These parameters are summarized in Table 2.2 [11].

Transmission BW		1.25 MHz	2.5 MHz	5 MHz	10 MHz	15 MHz	20MHz
Sub-carrier Duration T_{sub}		0.5ms					
Sub-carrier Spacing f_{space}		15kHz					
Sampling Frequency f_s		1.92 MHz	3.84MHz	7.68 MHz	15.36MHz	23.04 MHz	30.72 MHz
FFT and N_{IFFT}		128	256	512	1042	1536	2048
Number of occupied sub--carries N_{BW}		75	150	300	600	900	1200
Number of OFDM symbols per Sub-frame Short/Long (CP)		7/6					
CP Length (μs / sample)	***short***	(4.69/9)×6 (5.21/10)×1	(4.69/18)×6 (5.21/20)×1	(4.69/18)×6 (5.21/40)×1	(4.69/72)×6 (5.21/80)×1	(4.69/108)×6 (5.21/120)×1	(4.69/144)×6 (5.21/160)×1
	Long	(16.67/32)	(16.67/64)	(16.67/128)	(16.67/256)	(16.67/384)	(16.67/512)

Table 2.2 LTE Downlink Parameters

2.7) Multiple Antenna Techniques

Broadly, multiple antenna techniques utilize multiple antennas at the transmitter or/and receiver in combination with adaptive signal processing to provide smart array processing, diversity combining or spatial multiplexing capability of wireless system [10,12]. Previously, in conventional signal antenna systems the exploited dimensions are only time and frequency whereas multiple antenna systems exploit an additional spatial dimension. The utilization of spatial dimension with multiple antenna techniques fulfills the requirements of LTE; improved coverage

(possibility for larger cells), improved system capacity (more user/cell), QoS and targeted date rates are attained by using multiple antenna techniques as described in [13]. Multiple antenna techniques are the integrated part of LTE specifications because some requirements such as user peak data rates cannot be achieved without the utilization of multiple antenna schemes.

The radio link is influenced by the multipath fading phenomena due to constructive and destructive interferences at the receiver. By applying multiple antennas at the transmitter or at the receiver, multiple radio paths are established between each transmitting and receiving antenna. In this way dissimilar paths will experience uncorrelated fading. To have uncorrelated fading paths, the relative location of antennas in the multiple antenna configurations should be distant from each other. Alternatively, for correlated fading (instantaneous fading) antenna arrays are closely separated. Whether uncorrelated fading or correlated fading is required depends on what is to be attained with the multiple antenna configurations (diversity, beam-forming, or spatial multiplexing) [10]. Generally, multiple antenna techniques can be divided into three categories (schemes) depending on their different benefits; spatial diversity, beam-forming and spatial multiplexing which will be discussed further in the following sections.

2.7.1) Spatial Diversity

Conventionally, the multiple antennas are exercised to achieve increased diversity to encounter the effects of instantaneous fading on the signal propagating through the multipath channel. The basic principle behind the spatial diversity is that each transmitter and receiver antenna pair establishes a single path from the transmitter to the receiver to provide multiple copies of the transmitted signal to obtain an improved BER performance [14]. In order to achieve large gains with multiple antennas there should be low fading correlation between the

transmitting and the receiving antennas. Low value of correlation can be achieved when inter-antenna spacing is kept large. It is difficult to place multiple antennas on a mobile device due size restrictions depending upon the operating carrier frequency. An alternative solution is to use antenna arrays with cross polarizations, i.e., antenna arrays with orthogonal polarizations. The number of uncorrelated branches (paths) available at the transmitter or at the receiver refers to the diversity order and the increase in diversity order exponentially decreases with the probability of losing the signal. To achieve spatial diversity for the enhancement of converge or link robustness multiple antennas can be used either at the transmitter side or at the receiver side. We will discuss both transmit diversity where multiple antennas are used at the transmitter (MISO-multiple-input signal-output), and receive diversity using multiple receive antenna (SIMO signal-input multiple-output). On the other hand, MIMO channel provides diversity as well as additional degree of freedom for communication.

2.7.1.1) Receive Diversity

The receive diversity is the most straightforward and commonly utilized multiple antenna configuration which relies on the use of $N_r \geq 2$ (number of receive antennas) antennas at the receiver to achieve spatial diversity. Receive antenna diversity will improve system performance when the signals from different antennas are optimally combined in such a way that the resulting signal demonstrates a reduced amplitude variations when compared to the signal amplitude from any one antenna. Here diversity order is equal to the number of receive antennas in SIMO configuration and it collects more energy at the receiver to improve signal to noise ratio as compared to SISO (signal input signal output) configuration. Receive diversity configuration is depicted in figure 2.5. Two different combining methods are used to implement receive diversity (e.g., selection combining and gain combining). In selection combining, the branch with

the highest SNR is selected by the combiner for detection and in gain combining the linear combination of all branches is used for detection [16].

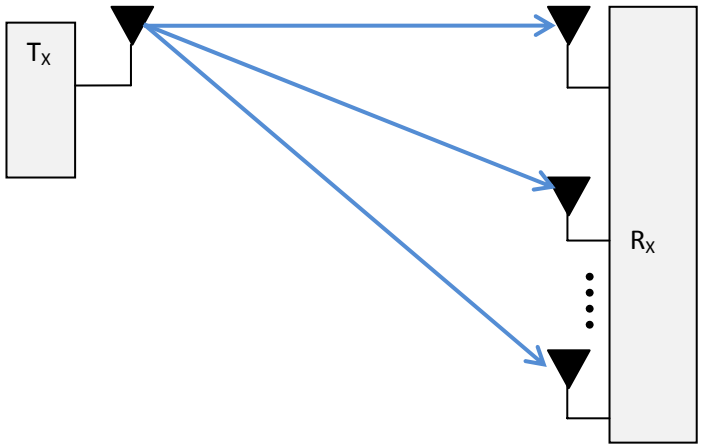

Figure 2.5: Receive diversity configurations

Receive diversity is an uncomplicated possibility to boost the link reliability but it becomes limited when the size of the receiver is small. In mobile radio communications the size of cell phones is becoming smaller and smaller so it is very hard task to place several antennas with enough spacing on such a small device to achieve uncorrelated channels [17]. For further study on receive diversity and different combining methods related to SIMO systems can be found in [10, 15, 16, 17, 18].

2.7.1.2) Transmit Diversity

The transmit diversity scheme relies on the use of $N_t \geq 2$ antennas at the transmitter side in combination with pre-coding in order to achieve spatial diversity when transmitting a single data stream [4,19]. Usually transmit diversity necessitates the absolute channel information at the transmitter but it becomes feasible to implement transmit diversity without the knowledge of the channel

with space time block coding [19]. The simplest of the diversity techniques is Alamouti space time coding (STC) scheme [20]. Transmit diversity configuration is illustrated in figure 2.6.

The use of transmit diversity is common in the downlink of cellular systems because it is cheaper and easy to install multiple antennas at base station than to put multiple antennas at every handheld device. In transmit diversity to combat instantaneous fading and to achieve considerable gain in instantaneous SNR, the receiver is being provided with multiple copies of the transmitted signal. Hence transmit diversity is applied to have extended converge and better link quality when the users experience terrible channel conditions.

In LTE, transmit diversity is defined only for 2 and 4 transmit antennas and these antennas usually need to be uncorrelated to take full advantage of diversity gain. As discussed in section 1, to achieve low mutual correlation between signal paths (channels) antennas have to be sufficiently separated relative to the carrier wavelength or should have different polarizations [9].

LTE physical layer supports both open loop and closed loop diversity schemes. In open loop scheme channel state information (CSI) is not required at the transmitter, consequently multiple antennas cannot provide beam-forming, only diversity gain can be achieved. On the other hand, closed loop scheme does not entail channel state information (CSI) at transmitter and it provides both spatial diversity and beam-forming as well.

By employing cyclic delay diversity and space frequency block coding, open loop transmit diversity can be accomplished in LTE. In addition, LTE also implements close loop transmit diversity schemes such as beam-forming.

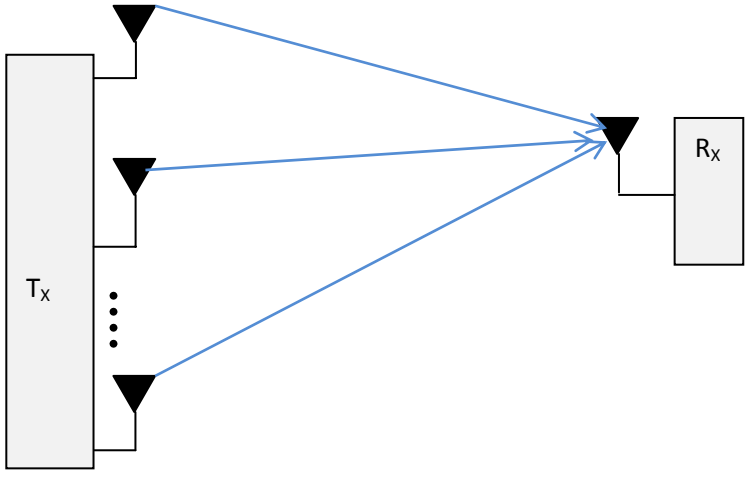

Figure 2.6: Transmit diversity configurations

2.7.1.3) Cyclic Delay Diversity (CDD)

In delay diversity, delayed replicas of the same signal are transmitted from different antennas at the base station in order to achieve diversity. If the channel is not time dispersive in itself, delay diversity is used to transform antenna diversity into frequency diversity. The use of delay diversity is completely transparent to the mobile terminal, which only observes single radio link with supplementary frequency selectivity [9,21]. Cyclic delay diversity (CDD) is the edition of generalized delay diversity (GDD) which is used to increase channel frequency selectivity as seen by the receiver in OFDM system [22]. The CDD operates blocks-wise that's why it is applicable for OFDM based system[1]. In cyclic delay diversity circularly delayed copies of the identical set of OFDM symbols on the identical set of OFDM subcarriers are transmitted from different transmit antennas. In order to attain cyclic delay (instead of linear delay) over the Fast Fourier Transform (FTT) size, a delay is introduced before the CP. The cyclic delay is added before the CP so that any value of delay can be employed without

[1] OFDM is a block base transmission scheme

changing the delay spread of the channel. Accumulation of cyclic time delay is equivalent to applying the phase shift in frequency domain before OFDM modulation as demonstrated in figure 7b where S_j corresponds to the complex modulated symbols which are mapped on 1^{st} antenna and phase shifted version of the same modulated symbols are mapped on 2^{nd} antenna. The use of the same delay to all sub-carriers in time domain results in linearly increasing phase shift across the sub-carriers with increasing subcarriers frequency. Different sub-carriers follow different spatial paths through multipath channel which gives rise diversity effect and increased frequency selectivity. For further reading on CDD [9, 16,22]. The general principle of CDD for two antenna configuration can be depicted in figure 2.7a [4].

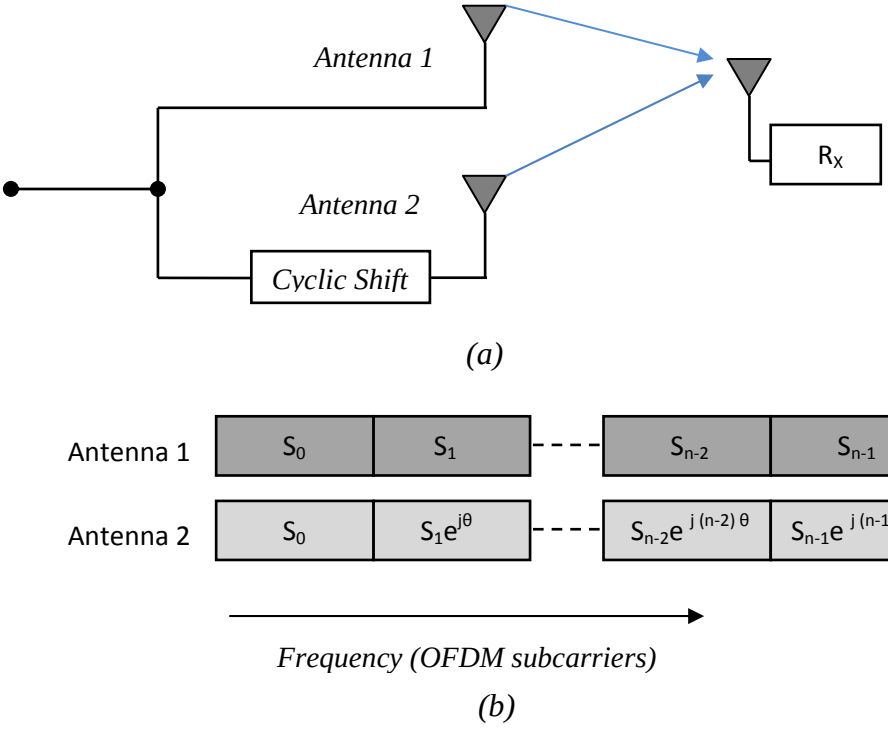

Figure 2.7: CDD for two antenna configuration

2.7.1.4) Space Frequency Block Coding (SFBC)

In LTE, transmit diversity is implemented by using Space Frequency Block Coding (SFBC). SFBC is a frequency domain adaptation of renowned Space-time Block Coding (STBC) where encoding is done in antenna/frequency domains rather than in antenna/time domains. STBC is also recognized as Alamouti coding [23]. So this SFBC is merely appropriate to OFDM and other frequency domain based transmission schemes.

The advantage of SFBC over STBC is that in SFBC coding is done across the sub-carriers within the interval of OFDM symbol while STBC applies coding across the number of OFDM symbols equivalent to number of transmit antennas [23]. The implementation of STBC is not clear-cut in LTE as it operates on the pairs of adjacent symbols in time domain while in LTE number of available OFDM symbols in a sub-frame is often odd. The operation of SFBC is carried out on pair of complex valued modulation symbols. Hence, each pair of modulation symbols are mapped directly to OFDM subcarriers of first antenna while mapping of each pair of symbols to corresponding subcarriers of second antenna are reversely ordered, complex conjugated and signed reversed as shown in figure 2.8.

For appropriate reception, mobile unit should be notified about SFBC transmission and linear operation has to be applied to the received signal. The dissimilarity between CDD and SFBC lies in how pairs of symbols are mapped to second antenna. Contrarily to CDD, SFBC grants diversity on modulation symbol level while CDD must rely on channel coding in combination with frequency domain interleaving to provide diversity in the case of OFDM [4,10].

The symbols transmitted from two transmitted antennas on every pair of neighboring subcarriers are characterized in [9] as follows:

$$X = \begin{bmatrix} x^{(0)}(1) & x^{(1)}(1) \\ x^{(0)}(2) & x^{(1)}(2) \end{bmatrix} = \begin{bmatrix} S_0 & -S_1{}^* \\ S_1 & S_0{}^* \end{bmatrix} \begin{matrix} \xrightarrow{\text{Space}} \\ \downarrow \text{Frequency} \end{matrix} \qquad 2.1$$

where $x^{(p)}(k)$ denotes the symbols transmitted from antenna port 'p' on the k^{th} subcarrier. The received symbol can be expressed as follows:

$$y = Hs + n \qquad 2.2$$

$$\begin{bmatrix} y_0 \\ y_1^* \end{bmatrix} = \frac{1}{\sqrt{2}} \begin{bmatrix} h_{00} & -h_{01} \\ h_{11}^* & h_{10}^* \end{bmatrix} \begin{bmatrix} S_0 \\ S_1^* \end{bmatrix} + \begin{bmatrix} n_0 \\ n_1^* \end{bmatrix} \qquad 2.3$$

where h_{ij} channel response of at symbol $'i'$ transmitted from antenna$'j'$, and $'n'$ is the additive white Gaussian noise.

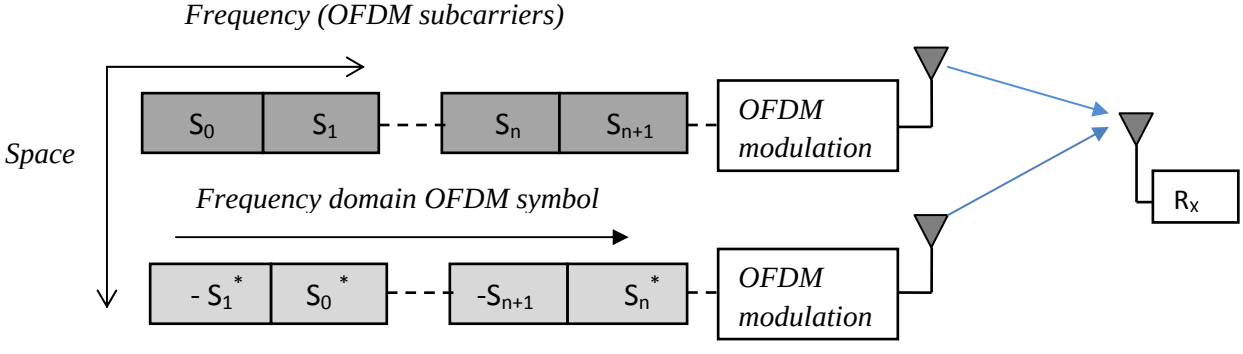

Figure 2.8: Space Frequency Block Coding SFBC assuming two antennas

2.7.2) Spatial Multiplexing

The use of multiple antennas at both the transmitter and the receiver can benefit from multipath fading to provide additional diversity and to improve signal-to-noise ratio compared to SISO systems. This advantage of multiple antennas can be used to provide higher data rates by efficient utilization of SNR over the air

interface, by the technique so-called spatial multiplexing. Spatial multiplexing can provide substantial increase in data rates by transmitting different data streams over different parallel channels provided by the multiple transmit and receive antennas, while using the same bandwidth and with no additional power expenditure. It is only possible in MIMO channels [24]. In MIMO systems, increase in capacity is linearly related to the number of the transmit/receive antenna pair. Consider a MIMO system with M transmit and N receive antennas, the radio channel for this system will consist of *M×N* ideally uncorrelated paths, as illustrated in Figure 2.9. This configuration offers $L = min\,(M, N)$ parallel channels that permit simultaneously transmission of *L* data streams and the receiver signal-to-noise ratio can be made to increase in proportion to the product $M \times N.$ A single bit stream is split into two half-rate bit streams, modulated and transmitted simultaneously from both antennas which can cause interference to each other at the receiver, and hence spatially multiplexed streams are overlapped due to propagation through the multipath channel. Therefore at the receiver side inference cancellation is employed to separate the different transmitted signals. For spatial multiplexing technique several decoding algorithms are developed for interference cancellation for the narrowband frequency flat fading case. In a low-complexity receiver, MMSE technique is employed which is discussed in details in chapter 5. According to Figure 2.9, received signals can be expressed as in [10]:

$$y = \begin{bmatrix} y_0 \\ y_1 \end{bmatrix} = \begin{bmatrix} h_{00} & h_{01} \\ h_{10} & h_{11} \end{bmatrix} \begin{bmatrix} S_0 \\ S_1 \end{bmatrix} + \begin{bmatrix} n_0 \\ n_1 \end{bmatrix} = H.s + n \qquad 2.4$$

where *H* is 2×2 channel matrix '*s*' represents the transmitted data symbols and *n* is 2×2 noise vector.

The spatial signatures of the two signals are well separated under the favorable channel circumstances. The receiver having the knowledge about channel

statistics can differentiate and recover data symbols s_0 and s_1. Assuming no noise, the estimates of data symbols s_0 and s_1 from the received signal and the channel coefficients can be obtained as follows:

$$s = \begin{bmatrix} s_0 \\ s_1 \end{bmatrix} = B \begin{bmatrix} h_{00} & -h_{01} \\ -h_{10} & h_{11} \end{bmatrix} \begin{bmatrix} y_0 \\ y_1 \end{bmatrix} \qquad 2.5$$

$$Where\ B = \frac{1}{h_{00}h_{11} - h_{01}h_{10}}$$

All sub-streams are multiplexed into original symbols stream after decoding. In addition, different parallel channels can be made independent of each other if some knowledge of the channel is available at the transmitter, thus by using closed-loop spatial multiplexing interfering signals at the receiver are significantly reduced. Further details about spatial multiplexing can be found in [4, 9, 10, 18].

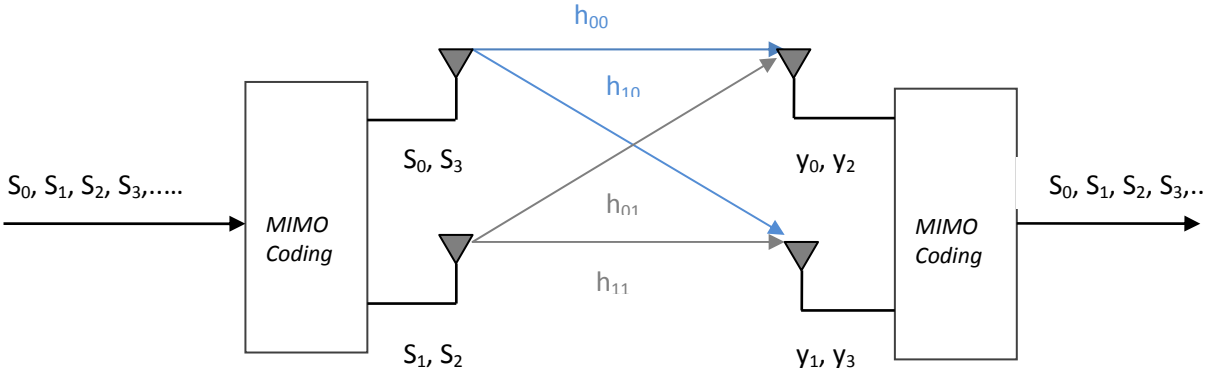

Figure 2.9: 2×2 Antenna Configuration (Here *M*=*N*=2)

2.7.3) Beam-forming

In general, beam-forming can be defined as the shaping of overall antenna beam in the direction of target receiving antenna to increase the signal strength at the

receiver in proportion to the number of transmit antennas. The Multiple antennas can provide beam-forming in addition to spatial diversity if some knowledge of relative channel phases is available at the transmitter which is not a requirement for spatial diversity and spatial multiplexing techniques.

In multiple antenna transmission schemes, beam forming can be employed on the basis of low and high mutual antenna correlation. In high mutual antenna correlation scheme the separation between antennas is relatively small as illustrated in Figure 2.10a and the overall transmission beam can be steered in different direction by applying different phase shifts to the signal to be transmitted. With different phase shifts applied to antennas having high mutual correlation is sometimes referred as classical beam-forming which cannot provide any diversity against radio channel fading but just an increase in the received signal strength. In conventional beam-forming to achieve optimal SNR over wireless link the same date symbol is transmitted simultaneously from different antennas after a complex weight is applied to each signal path with the aim of steering the antenna array [10, 18].

Low mutual antenna correlation usually involves either a large antenna separation as depicted in Figure 2.10b or different antenna polarizations. However, in this case each antenna transmits simultaneously a general complex[2] value weighted combination of two data symbols. Due to low mutual antenna correlation each antenna may experience different channel instantaneous gains and phases.
The different complex weights (pre-coding matrix) are applied to symbols $S_0, S_1, S_2, S_3, \ldots$ to be transmitted from different antennas. After applying pre-coding weights, two separate data streams are transmitted from two different antennas simultaneously as spatial multiplexing. As illustrated in Figure 2.10b, the

[2] General Complex means both amplitude and phase of the signal to be transmitted on different antennas.

data symbol x_0 is transmitted from the upper antenna during first symbol time which is a linear combination of two data symbols, s_0 and s_1. During the same time, data symbol x_1 is transmitted with different combinations of the same data symbols from the lower antenna, thus efficiently doubling-up the data rate. So the relation between the transmitted data and the input symbols is demonstrated as follows:

$$X = \begin{bmatrix} x_0 \\ x_1 \end{bmatrix} = \begin{bmatrix} w_{00} & w_{01} \\ w_{10} & w_{11} \end{bmatrix} \begin{bmatrix} s_0 \\ s_1 \end{bmatrix} = W.s \qquad 2.6$$

where W corresponds 2×2 pre-coding matrix and 's' corresponds 2×1 transmitted symbols matrix.

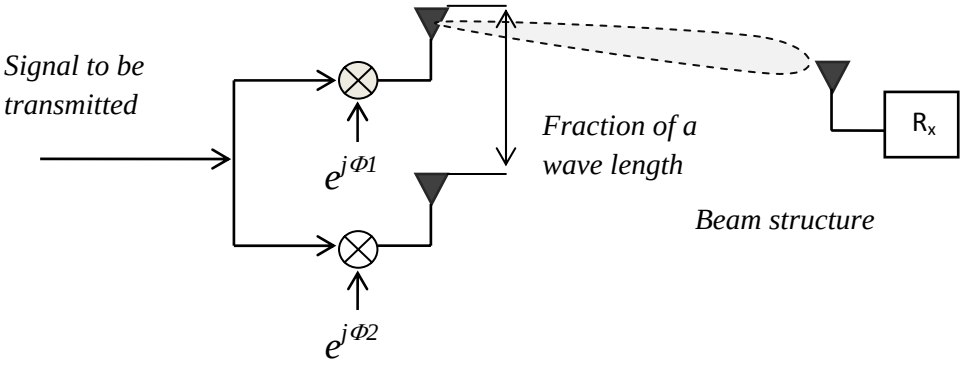

Figure 2.10a: Classical beam-forming with high mutual antenna correlation

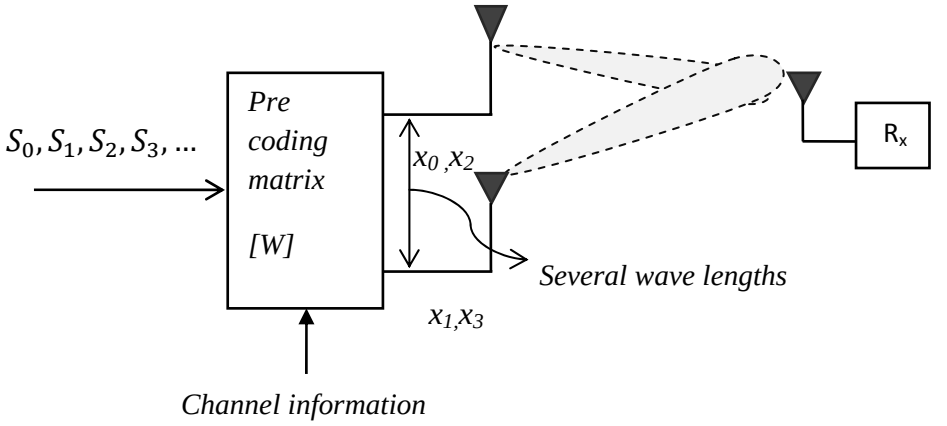

Figure 2.10b: Pre-coder based beam-forming in case of low mutual antenna correlation

Chapter 3 LTE Downlink System Model

3.1) Introduction

To give a detailed description of LTE downlink, system model based on multiple antenna transmission schemes and OFDM is the motivating force in the writing of this chapter. The combination of new technologies, i.e., MIMO-OFDM is employed to fulfill the LTE radio interface requirements [25]. MIMO techniques discussed in Chapter 2 have been considered as the key approach for providing required bandwidth efficiency and high data rates in the evolution of future generation mobile communication systems. On the other-hand, OFDM is the special case multicarrier transmission scheme which is extremely attractive to implement multicarrier modulation schemes to combat ISI in multipath fading environments with high spectral efficiency for LTE downlink transmission. OFDM uses multiple overlapping but orthogonal carrier signals instead of single carrier to achieve high spectral efficiency and high data rates. The LTE downlink system model used in simulation is depicted in Figure 3.1 with two transmit and two receive antennas.

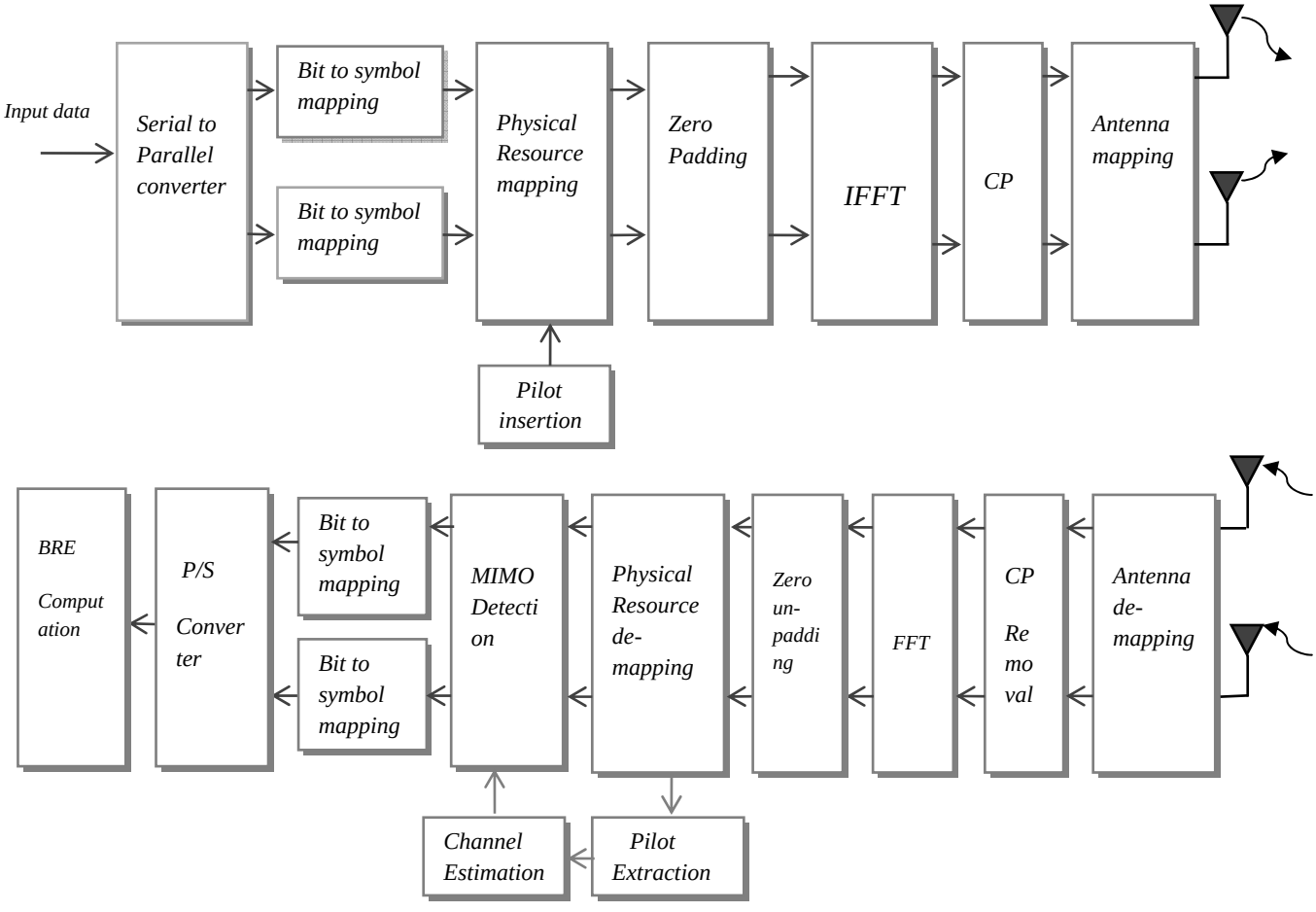

Figure 3.1 LTE Downlink system model with 2×2 MIMO

3.2) General Description

In LTE downlink transmission, OFDM symbols are generated by performing different manipulations on the single binary input data stream as shown in Figure 3.1.

In first step single binary input data stream is converted into two parallel data streams by the serial to parallel converter. Following each parallel data stream is modulated with different subcarriers frequency by using different constellation

mapping schemes (QPSK, 16QAM, 64QAM) defined in [26]. The Constellation mapping is a way of assigning sinusoids having unique amplitude and/or phase to the input binary data. These higher modulation or constellation schemes are required to achieve bandwidth efficiency and high data rates in LTE.

Subsequently, according to LTE downlink sub-frame structure as described in chapter 2 the complex constellation symbols of each data stream and pilot symbols are mapped on OFDM resource gird. The different pilot symbols arrangement for each antenna is used for the purpose of channel estimation as documented in [27]. After the physical resource mapping zero padding is done because the sampling rate is much higher than the transmission bandwidth of the system. In zero padding the length of the signal spectrum is increased by specific number of zeros. The zero padded signals are applied to IFFT block for the sake of OFDM modulation. In OFDM modulation the serial input data stream is divided into a number of parallel streams and then these low-rate parallel streams are transmitted over different subcarriers simultaneously. The minimum frequency separation is required between these subcarriers to maintain orthogonality of their corresponding time domain wave forms. In frequency domain these different subcarriers overlap. Thus, available bandwidth is used in efficient way. IFFT is an efficient algorithm used to generate an OFDM symbols and in complexity reduction of the transmitter. Finally CPs are inserted before the transmission to OFDM modulated signal. If channel is not time-dispersive, the transmitted OFDM signal can be demodulated without any interference. On the other hand if the channel is time dispersive then the Orthogonality will be lost between the subcarriers because of the overlapping of the correlation interval of the demodulator for one path with the symbol interval of the other paths. This will result in inter-symbol interference as well as inter-carrier interference. To combat these interferences and to overcome time dispersion of radio channel, CP is used

in OFDM system. For further reading on OFDM working, details can be seen in [28].

The receiver side basically performs the reverse operation of the transmitter with some additional operations (e.g., channel estimation) in order to find the estimates of multipath channel to recover information properly [25]. In the first step, cyclic prefixes are removed from the received data symbols. FFT is performed to recover the modulated symbol values of all subcarriers and to convert the received signal into frequency domain. To perform channel estimation (see chapter 5), reference symbols are extracted from each sub-frame. To recover original data streams, the received complex symbols from both antennas are delivered to MIMO detection stage. After this the complex constellation symbols are de-mapped into binary values and this parallel data is converted in serial data to find out the estimates of the transmitted data [25].

CHAPTER 4 Radio Propagation Models

4.1) Introduction

From the beginning wireless communications there is a high demand for realistic mobile fading channels. The reason for this importance is that efficient channel models are essential for the analysis, design, and deployment of communication system for reliable transfer of information between two parties. Correct channel models are also significant for testing, parameter optimization and performance evolution of communication systems. The performance and complexity of signal processing algorithms, transceiver designs and smart antennas etc., employed in future mobile communication systems, are highly dependent on design methods used to model mobile fading channels. Therefore, correct knowledge of mobile fading channels is a central prerequisite for the design of wireless communication systems [29, 30, 31].

The difficulties in modeling a wireless channel are due to complex propagation processes. A transmitted signal arrives at the receiver through different propagation mechanisms shown in figure 4.1. The propagation mechanisms involve the following basic mechanisms: i) free space or line of sight propagation ii) specular reflection due to interaction of electromagnetic waves with plane and smooth surfaces which have large dimensions as compared to the wavelength of interacting electromagnetic waves iii) Diffraction caused by bending of electromagnetic waves around corners of buildings iv) Diffusion or scattering due to contacts with objects having irregular surfaces or shapes with sizes of the order of wavelength v) Transmission through objects which cause partial absorption of energy [16,29]. It is significant here to note that the level of information about the

environment a channel model must provide is highly dependent on the category of communication system under assessment. To predict the performance of narrowband receivers, classical channel models which provide information about signal power level distributions and Doppler shifts of the received signals, may be sufficient. The advanced technologies, (e.g., UMTS and LTE) build on the typical understanding of Doppler spread and fading; also incorporate new concepts such as time delay spread, direction of departures (DOD), direction of arrivals (DOA) and adaptive array antenna geometry [30]. The presence of multipaths (multiple scattered paths) with different delays, attenuations, DOD and DOA gives rise to highly complex multipath propagation channel.

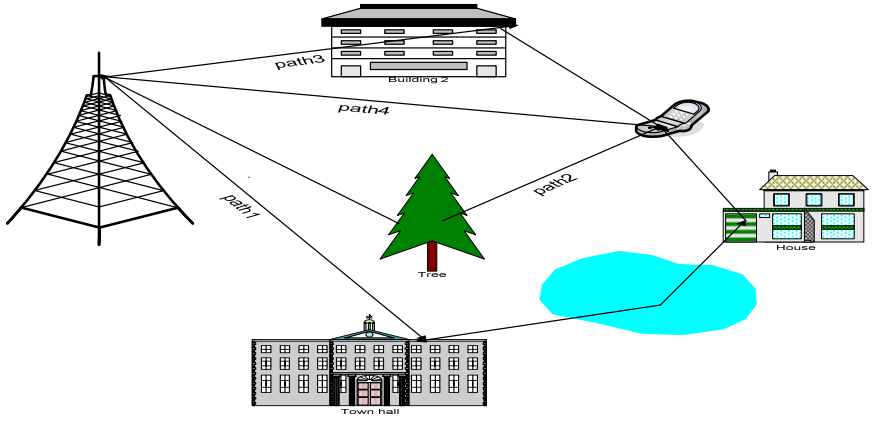

Figure 4.1: Signal propagation through different paths showing multipath propagation phenomena

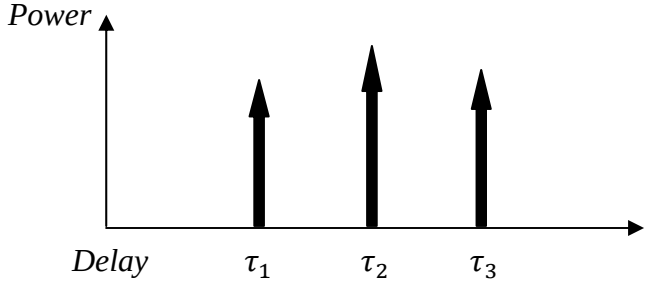

Figure 4.2: Power delay profile of a multipath channel

4.2) Multipath Propagation Channel

Multipath signals arrive at the receiver with different propagation path lengths called multipath taps. The different propagation path lengths cause different propagation time delays. Figure 4.2 illustrates power delay profile (PDP) of a multipath channel with three distinct paths. Depending on the phases the multipath signals interact either constructively or destructively at the receiver. This makes power of channel taps time varying resulting in fading dips as shown in figure 4.3. The power distribution of channel taps is described by a distribution function depending on the propagation environment. The most severe multipath channel is Rayleigh fading channel in which there is no line of sight path and the channel taps are independent. In the case of Rician fading channel the fading dips are low due to the presence of line of sight component in addition to the dispersed paths. A radio channel can be characterized as narrowband or wideband depending on the channel characteristics and duration of a symbol. Due to above propagation mechanisms, the impulse response of a multipath channel consists of a series of pulses spread in time or frequency. If the time difference between the first and the last pulse is smaller than the duration of a symbol, then the system is called narrowband system. If the time difference between the first and last pulse is greater than the duration of a symbol, then the system is called wideband system. Wideband characteristics of impulse response are often used to describe the behavior of the multipath channel.

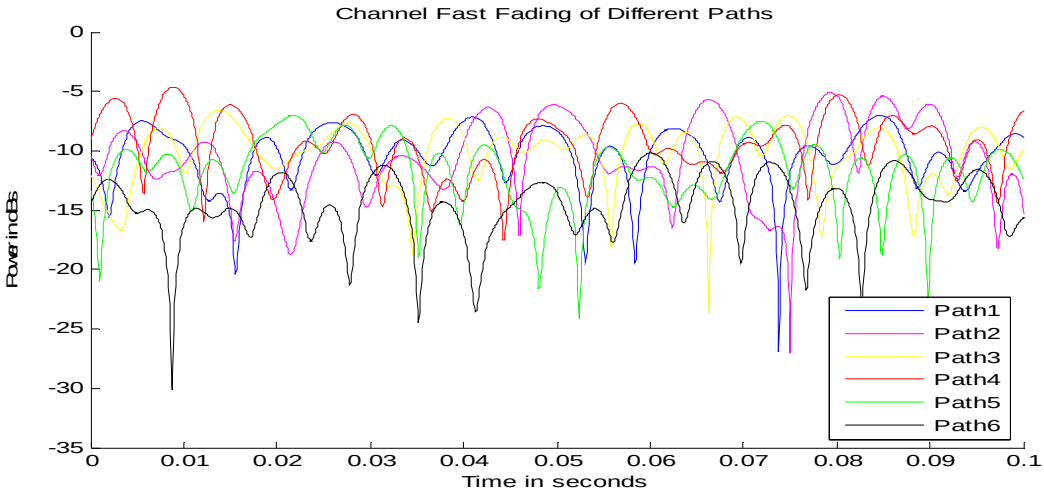

Figure 4.3: Received signal power level of a time varying multipath propagation channel

The degradation in the received signal level due to multipath effects can be classified into large scale path loss component, medium scale slow varying component with log-normal distribution and small scale fast fading component with Rayleigh or Rician distribution depending on the absence or presence of LOS component between the transmitter and receiver [29]. Thus, a three stage propagation model can be used to describe a wireless cellular environment.

4.2.1) Large Scale Propagation Model

Large scale propagation model is used to characterize the received signal strength by averaging the amplitude or power level of the received signal over large transmitter-receiver separation distances in the range of hundreds or thousands of a wavelength. The large scale models are often derived from measured data. However, semi-empirical models are employed in smaller areas to achieve higher accuracy. The theoretical models are used which are then fitted to measured data to obtain desired model for a particular propagation scenario.

4.2.2) Medium Scale Propagation Model

Medium scale propagation model determines the gradual variations of the local mean amplitude or the local mean power of the received signal over a time-variant multipath channel when the mobile station moves over distances larger than a few tens or hundreds of a wavelength. Some existing components will disappear while new components will appear. For narrowband measurements, it is observed that variations of the local mean power of the received signal follow log-normal distribution which is called slow fading or shadowing. The mean and standard deviations are determined from large scale propagation model in the environment of interest. The shadowing is caused by obstructions like trees and foliage. The wideband channel is characterized by the time-variant channel impulse response.

$$h(t,\tau) = \sum_n a_n\,(t) e^{j\varphi_n(t)} \delta(\tau - \tau_n) \qquad 4.1$$

where a_n is the amplitude, φ is the phase and τ is the delay of the n^{th} component arriving at particular time t. The impulse response of wideband channel consists of series of independently fading paths received at different time delays. Each independent path of the wideband channel can be treated as narrowband channel with fading characterized by log-normal distribution.

4.2.3) Small Scale Propagation Model

This model is used to characterize the rapid variations of the received signal strength due to changes in phases when a mobile terminal moves over small distances on the order of a few wavelengths or over short time durations on the order of seconds. Since the mean power remains constant over these small distances, small scale fading can be considered as superimposed on large scale

fading for large scale models. The most common description of small scale fading is by means of Rayleigh distribution.

$$f_{\propto}(\propto) = \frac{\alpha}{\sigma^2} e^{-\frac{\propto^2}{2\sigma^2}} \qquad \propto \geq 0 \qquad 4.2$$

This distribution represents the sum of amplitudes of the same order of a large number of uncorrelated components with phases uniformly distributed in the interval (0, 2π). The parameter σ is the root mean square value of the received signal. In the case of line of sight component, the signal fading can be modeled using Rician distribution.

$$f_{\propto(\propto)=\frac{\propto}{\sigma^2}} I_o\left(\frac{\propto.\rho}{\sigma^2}\right) e^{-\frac{\propto^2+\rho^2}{2\sigma^2}} \qquad \propto \geq 0 \qquad 4.3$$

where I_o represents modified Bessel function of first kind and zero order, ρ is the amplitude of the line of sight component (LOS). If there is no LOS component, Rician distribution can be simply expressed as Rayleigh distribution.

In case of wideband modeling, each path of the impulse response can be modeled as Rayleigh distributed with uniform phase except LOS cases. In LOS, first path follows Rician distribution. A common method used of wideband channel models is tapped delay line model in which the taps follow above mentioned distributions.

4.3) Propagation aspects and Parameters

The behavior of a multipath channel needs to be characterized in order to model the channel. The concepts of Doppler spread, coherence time, and delay spread and coherence bandwidth are used describe various aspects of the multipath channel.

4.3.1) Delay Spread

To measure the performance capabilities of a wireless channel, the time dispersion or multipath delay spread related to small scale fading of the channel needs to be calculated in a convenient way. One simple measure of delay spread is the overall extent of path delays called the excess delay spread. This is only convenient way because different channels with the same excess delays can exhibit different power profiles which have more or less impact on the performance of the system under consideration. A more efficient method to determine channel delay spread is the root mean square (rms) delay spread (τ_{rms}) which is a statistical measure and gives the spread of delayed components about the mean value of the channel power delay profile. Mathematically, rms delay spread can be described as second central moment of the channel power delay profile [29] which is written as follows:

$$\tau_{rms} = \sqrt{\frac{\sum_{n=0}^{N-1} P_n(\tau_n - \tau_m)^2}{\sum_{n=0}^{N-1} P_n}} \qquad 4.4$$

where, $\tau_m = \frac{\sum_{n=0}^{N-1} P_n \tau_n}{\sum_{n=0}^{N-1} P_n}$ is the mean excess delay

4.3.2) Coherence Bandwidth

When the channel behavior is studied in frequency domain than coherence bandwidth $\Delta \mathrm{f_c}$ is of concern. The frequency band, in which the amplitudes of all frequency components of the transmitted signal are correlated, i.e., with equal gains and linear phases, is known as coherence bandwidth of that channel [30]. The channel behavior remains invariant over this bandwidth. The coherence bandwidth varies in inverse proportion to the delay spread. A multipath channel can be categorized as frequency flat fading or frequency selective fading in the following way.

Frequency flat fading: A channel is referred to as frequency flat if the coherence bandwidth $\Delta f_c \gg B$, where B is the signal bandwidth. All frequency components of the signal will experience the same amount of fading.

Frequency selective fading: A channel is referred to as frequency selective if the coherence bandwidth $\Delta f_c \leq B$. In this case different frequency components will undergo different amount of fading. The channel acts as a filter since the channel coherence bandwidth is less than the signal bandwidth; hence frequency selective fading takes place [32].

4.3.3) Doppler Spread

The Doppler spread arises due to the motion of mobile terminal. Due to the motion of mobile terminal through the standing wave the amplitude, phase and filtering applied to the transmitted signal vary with time according to the mobile speed [33]. For an unmodulated carrier, the output is time varying and has non-zero spectral width which is Doppler spread. For a single path between the mobile terminal and the base station, there will be zero Doppler spread with a simple shift of the carrier frequency (Doppler frequency shift) at the base station. The Doppler frequency depends on the angle of movement of the mobile terminal relative to the base station.

4.3.4) Coherence Time

The time over which the characteristics of a channel do not change significantly is termed as coherence time. The reciprocal of the Doppler shift is described as the coherence time of the channel. Mathematically we can describe coherence time as follows:

$\mathbf{T_c = \frac{1}{2.\pi.\upsilon_{rms}}}$, where υ_{rms} is root mean square vale of Doppler spread. The coherence time is related to the power control schemes, error correction and

interleaving schemes and to the design of channel estimation techniques at the receiver.

4.4) Standard Channel models

Standard channel models can be developed by setting up frame work for generic channel models and finding set of parameters that need to be determined for the description of the channel. The other method is to set up measurement campaigns and extracting numerical values of parameters and their statistical distributions [34].

When designing LTE, different requirements are considered; user equipment (UE) and base station (BS) performance requirements which are crucial part of LTE standards, Radio Resource Management (RRM) requirements to ensure that the available resources are used in an efficient way to provide end users the desired quality of service, the RF performance requirements to facilitate the existence of LTE with other systems (e.g., 2G/3G) systems [35]. The standard channel models play a vital role in the assessment of these requirements. In the following section, some standard channel models are discussed which are used in the design and evolution of the UMTS-LTE system.

4.4.1) SISO, SIMO and MISO Channel Models

COST projects, Advanced TDMA Mobile Access, UMTS Code Division Testbed (CODIT) conducted extensive measurement campaigns to create datasets for SISO, SIMO and MISO channel modeling and these efforts form the basis for ITU channel models which are used in the development and implementation of the third generation mobile communication systems [9]. COST stands for the “European Co-operation in the Field of Scientific and Technical Research”. Several Cost efforts were dedicated to the field of wireless communications, especially radio

propagation modeling, COST 207 for the development of Second Generation of Mobile Communications (GSM), COST 231 for GSM extension and Third Generation (UMTS) systems, COST 259 "Flexible personalized wireless communications (1996-2000)" and COST 273 "Towards mobile broadband multimedia networks (2001-2005)". These projects developed channel models based on extensive measurement campaigns including directional characteristics of radio propagation (Cost 259 and Cost 273) in macro, micro and picocells and are appropriate for simulations with smart antennas and MIMO systems. These channel models form the basis of ITU standards for channel models of Beyond 3G systems. Detailed study of COST projects can be found in [36, 37, 38].

The research projects ATDMA and CODIT were dedicated to wideband channel modeling specifically channel modeling for 3rd generation systems and the corresponding radio environments. The wideband channel models have been developed within CODIT using statistical-physical channel modeling approach while stored channel measurements are used in ATDMA which are complex impulse responses for different radio environments. The details of these projects can be found in [31].

4.4.2) MIMO Channel Models

Multiple-input multiple-output wireless communication techniques offer the promise of increased spectral efficiency throughput and quality of service for MIMO communication systems [39,40]. As an example, figure 4.5 shows that the capacity increases linearly with the increase in number of antennas. The performance of MIMO communication systems is highly dependent on the underlying propagation conditions. The spatial characteristics of a radio channel have significant effects on the performance of MIMO systems. The MIMO

techniques take the advantage of multipath effects in the form of spatial diversity to significantly improve SNR by combining the outputs of de-correlated antenna arrays with low mutual fading correlation. The other technique to increase the effective data rate of a MIMO system using multiple antenna arrays is spatial multiplexing which creates multiple parallel channels between the transmitter and the receiver sides. Multiple antennas at the transmitter and/or the receiver side can be used to shape the overall beam in the direction of a specific user to maximize the gain. This technique is called beam forming. Multiple antennas transmission techniques are described in details in chapter 2. The large MIMO gains can be achieved by low spatial correlation. The antenna separation, in terms of wavelength of the operating frequency, has significant impacts on the spatial correlation. To achieve low fading correlation, the antenna separation should be large. The small sizes of wireless devices restrict large antenna separation depending upon the wavelength of the operating frequency. An alternative solution to achieve low correlation is to use antenna arrays with cross Polarizations (i.e., antenna arrays with polarizations in orthogonal or near orthogonal orientations) [18,41].

4.4.3) Effect of Spatial Correlation on MIMO Performance

The MIMO transmission schemes, spatial diversity and spatial multiplexing, can substantially improve the performance and overcome the undesirable multipath effects if the spatial dimension is properly configured to leverage the richness of multipath environment [18,35,39]. The diversity gain can be achieved only when there is low correlation between the transmitting and the receiving antennas. The spatial correlation has also a significant impact on the capacity limits of a MIMO channel [9]. The capacity of a channel without channel knowledge at the transmitter can be determined as [35].

$$C = log\left[det\ (I_{N_R} + \frac{\gamma}{N_T} HH^H)\right] \qquad 4.5$$

Where,N_T and N_R are the number of transmit and receive antennas, respectively and I_{N_R} is the $N_R x N_R$ identity matrix. The symbol γ represents the signal to noise plus interference ratio (SINR) and *H* is the channel transfer function. The operator $\{\cdot\}^H$ represents the Hermitian transpose operation.

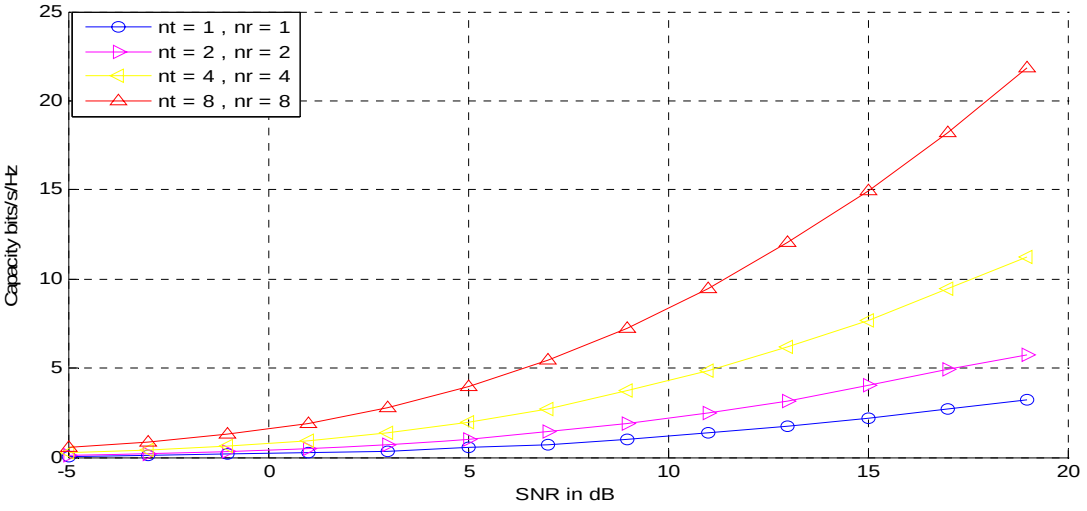

Figure 4.4: The increase in the capacity with the increase in number of antennas. The capacity of the system increases linearly with increasing number of antennas

It is obvious that for a given number of transmit antennas and signal to interference ratio, the spatial correlation value of MIMO channel determines the theoretical capacity limits. Figure 4.6 illustrates the impact of spatial correlation of the performance of radio link quality of MIMO channel. It illustrates the performance of system in terms of bit error rate. Alamouti space time coding is used with diversity order of 4 ($M_j M_i$=2x2=4) in flat fading Rayleigh channel with different correlation values. The results demonstrate that SNR required to support different values of bit error rate varies depending on different correlation values.

The diversity gain can be achieved by low correlation values. To achieve low correlation values, the separation between antenna arrays should be large.

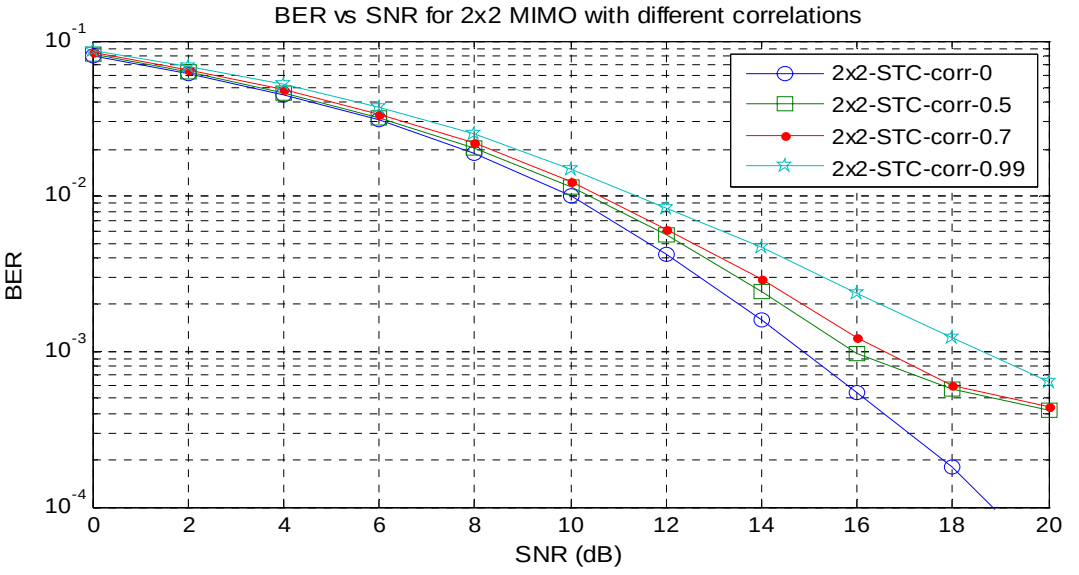

Figure 4.5: BER curves for 2x2 MIMO systems using flat fading Rayleigh channel with different correlation values which show that BER decreases with low correlation values

4.4.4) ITU Multipath Channel Models

The ITU standard multipath channel models proposed by ITU [42] used for the development of 3G 'IMT-2000' group of radio access systems are basically similar in structure to the 3GPP multipath channel models. The aim of these channel models is to develop standards that help system designers and network planners for system designs and performance verification. Instead of defining propagation models for all possible environments, ITU proposed a set of test environments in [42] that adequately span the all possible operating environments and user mobility. In our work we used ITU standard channel models for pedestrian and vehicular environments.

4.4.4.1) ITU Pedestrian-A, B

We used both Pedestrian-A and Pedestrian-B channel models in our work. The mobile speed is considered to be 3 km/h in each of these cases. For Pedestrian models the base stations with low antennas height are situated outdoors while the pedestrian user are located inside buildings or in open areas. Fading can follow Rayleigh or Rician distribution depending upon the location of the user. The number of taps in case of Pedestrian-A model is 3 while Pedestrian-B has 6 taps. The average powers and the relative delays for the taps of multipath channels based on ITU recommendations are given in table 4.1 [42].

Tap No	*Pedestrian-A*		*Pedestrian-B*		*Doppler Spectrum*
	Relative Delay (ns)	*Average Power(dB)*	*Relative Delay (ns)*	*Average Power(dB)*	
1	*0*	*0*	*0*	*0*	*Classical*
2	*110*	*-9.7*	*200*	*-0.9*	*Classical*
3	*190*	*-19.2*	*800*	*-4.9*	*Classical*
4	*410*	*-22.8*	*1200*	*-8*	*Classical*
5	*NA*	*NA*	*2300*	*-7.8*	*Classical*
6	*NA*	*NA*	*3700*	*-23.9*	*Classical*

Table 4.1: Average Powers and Relative Delays of ITU multipath Pedestrian-A and Pedestrian-B cases

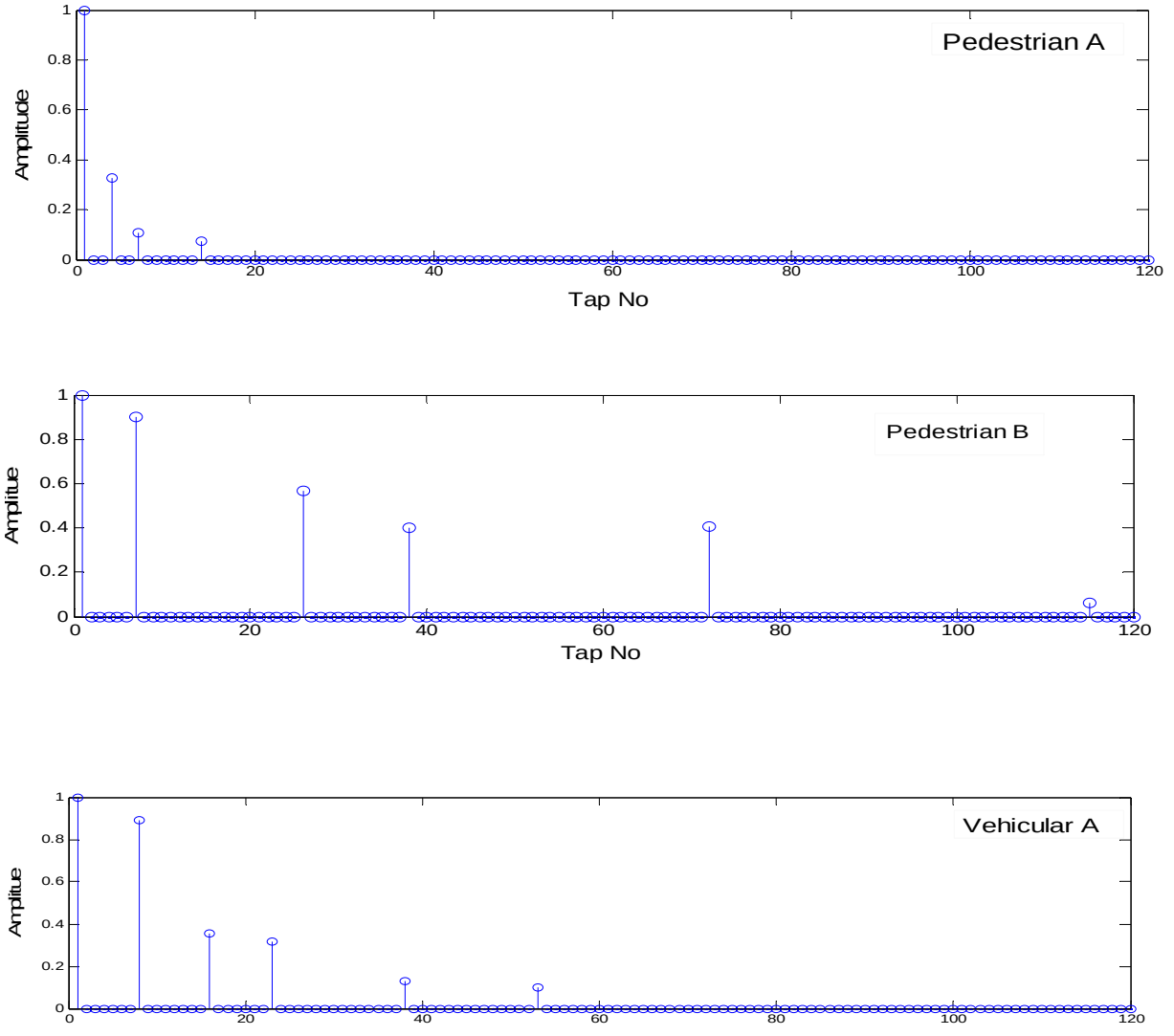

Figure 4.6: Channel Impulse Responses according to ITU standards which are to be used in simulations for channel estimation of LTE

4.4.4.2) ITU Vehicular-A (V-30, V-120 and V-350)

The vehicular environment is categorized by large macro cells with higher capacity, limited spectrum and large transmits power. The received signal is composed of multipath reflections without LOS component. The received signal power level

decreases with distance for which pass loss exponent varies between 3 and 5 in the case of urban and suburban areas. In rural areas path loss may be lower than previous while in mountainous areas, neglecting the path blockage, a path loss attenuation exponent closer to 2 may be appropriate.

For vehicular environments, we used the ITU vehicular-A channel models in our work. The mobile speed considered is 30 km/h, 120 km/h and 350 km/h. The propagation scenarios for LTE with speeds from 120 km/h to 350 km/h are also defined in [43] to model high speed scenarios (e.g., high speed train scenario at speed 350km/h). The maximum carrier frequency over all frequency bands is *f*=2690 MHz and the Doppler shift at speed *v*=350 km/h is 900 Hz. The average powers and the relative delays for the taps of multipath channels based on ITU recommendations are given in table 4.2 [42].

	Tap No					
Average Power(dB)	*0*	*-1.0*	*-9.0*	*-10.0*	*-15.0*	*-20.0*
Relative Delay(ns)	*0*	*310*	*710*	*1090*	*1730*	*2510*

Table 4.2: Average Powers and Relative Delays for ITU Vehicular-A Test Environment

4.4.5) Extended ITU models

The analysis done by ITU-R showed that evolution of 3G systems to future generation networks will require technology changes on large scale while new quality of service (QoS) requirements will require increased transmission bandwidth. So LTE channel models require more bandwidth as compared to UMTS channel models to account that fact that channel impulses are associated to the delay resolution of the receiver. The LTE channel models developed by 3GPP are

based on the existing 3GPP channel models and ITU channel models. The extended ITU models for LTE were given the name of Extended Pedestrian-A (EPA), Extended Vehicular-A (EVA) and Extended TU (ETU). These channel models are classified on the basis of low, medium and high delay spread where low delay spreads are used to model indoor environments with small cell sizes while medium and high delay spreads are used to model urban environments with large cells. The high delay spread models are according to Typical Urban GSM model [43]. The power delay profiles for these channel models are given in tables 4.3.1, 4.3.2 and 4.3.3, respectively [43].

	Tap No						
Average Power(dB)	*0.0*	*-1.0*	*-2.0*	*-3.0*	*-8.0*	*-17.2*	*-20.8*
Excess Delay(ns)	*0.0*	*30*	*70*	*80*	*110*	*190*	*410*

Table 4.3.1: Power Delay Profiles for Extended ITU Pedestrian-A Model

	Tap No								
Average Power(dB)	*0.0*	*-1.5*	*-1.4*	*-3.6*	*-0.6*	*-9.1*	*-7.0*	*-12*	*-16.9*
Excess Delay(ns)	*0.0*	*30*	*150*	*310*	*370*	*710*	*1090*	*1730*	*2510*

Table 4.3.2: Power Delay Profiles for Extended ITU Vehicular-A Model

	Tap No								
Average Power(dB)	*-1.0*	*-1.0*	*-1.0*	*0.0*	*0.0*	*0.0*	*-3.0*	*-5.0*	*-7.0*
Excess Delay(ns)	*0.0*	*50*	*120*	*200*	*230*	*500*	*1600*	*2300*	*5000*

Table 4.3.3: Power Delay Profiles for Extended Typical Urban Model

The above Extended ITU Models are also used in this work. The Doppler frequencies for these channel models are defined in a similar way to that of EUTRA. The Doppler frequencies for LTE channel models with low, medium and high Doppler conditions are 5Hz, 70Hz and 900Hz respectively [43]. The following combinations of delay spread and Doppler spread are proposed in [43]; extended pedestrian-A 5 Hz, extended vehicular-A 5Hz, Extended Vehicular-A 70 Hz and Extended Typical Urban 70 Hz.

Chapter 5 Channel Estimation in LTE

5.1) Introduction

In this chapter, channel estimation techniques used in LTE down link are described. Channel estimation is a vital part of receivers designs used in mobile communication systems. The effect of the channel on the transmitted information must be estimated in order to recover the transmitted information correctly. The estimation of channel effects is often based on an approximate underlying model of the radio propagation channel [44]. The receiver can precisely recover the transmitted information as long as it can keep track of the varying radio propagation channels. Channel models are described in the chapter 4.

5.2) Signal Model

In this work, we consider one OFDM symbol to perform channel estimation in LTE down link. For the purpose of channel estimation we consider the channel frequency response vector and a diagonal matrix containing the transmitted frequency domain samples as follows:

$$Y = XH + \mu \qquad 5.1$$

where $X \epsilon C^{N_{IFFT} \times N_{IFFT}}$ is a diagonal matrix with transmitted data samples, reference symbols or zeros, $H \epsilon C^{N_{IFFT}}$ contains unknown channel frequency response coefficients to be estimated and $\mu \epsilon C^{N_{IFFT}}$ is the noise vector. The channel frequency response (CFR) can be expressed in terms of channel impulse response (CIR) as $H = Fh.$ So the channel impulse response can be written as follows [45]:

$$Y = XFh + \mu \qquad 5.2$$

In above equation $F \epsilon C^{N_{IFFT} \times N_{IFFT}}$ is DFT matrix which can be written as follows:

$$\begin{bmatrix} f_{(1,1)} & \cdots & f_{(1,N_{IFFT})} \\ \vdots & \ddots & \vdots \\ f_{(N_{IFFT},1)} & \cdots & f_{(N_{IFFT},N_{IFFT})} \end{bmatrix} \qquad 5.3$$

The channel estimation is done using transmitted reference symbols, which are inserted among data subcarriers as per design specifications of 3GPP LTE [3]. The reference symbols structure is discussed in chapter 2. Before introducing channel estimation schemes we consider some simplifications in our signal structure in order to reduce complexity of the estimator [45].

- Only the channel taps with significant energy are considered. So we consider first *L* columns (where *L* represents the length of the channel) of the matrix *F* corresponding to the maximum delay at tap *L-1*.
- The reference symbols are slotted in according to LTE design specifications so, only rows of the matrix *F* corresponding to the position of these reference symbols are considered for the diagonal matrix *X*. Now equation 2 can be written as:

$$Y = X_r T_r h + \mu_r \qquad 5.4$$

where, $X_r \epsilon C^{N_r \times N_r}$ is a diagonal matrix containing reference symbols. The vector *Y* is the output and $\mu_r \epsilon C^{N_r \mathrm{x} L}$ is the truncated white Gaussian noise. The vector $h \epsilon C^{N_r \mathrm{x} L}$ represents the unknown CIR coefficients to be estimated. The matrix $T_r \epsilon C^{N_r \times L}$ is a Fourier matrix associated with transmitted reference symbols which can be written as follows:

$$T_r = \frac{1}{\sqrt{N_{DFT}}}\begin{bmatrix} e^{-j\omega(i_r)(0)} & e^{-j\omega(i_r)(1)} & \dots & e^{-j\omega(i_r)(L-1)} \\ e^{-j\omega(i_r+1)(0)} & e^{-j\omega(i_r+1)(1)} & \dots & e^{-j\omega(i_r+1)(L-1)} \\ \vdots & \vdots & \ddots & \vdots \\ \vdots & \vdots & \ddots & \vdots \\ e^{-j\omega(i_r+N_r-1)(0)} & e^{-j\omega(i_r+N_r-1)(1)} & \dots & e^{-j\omega(i_r+N_r-1)(L-1)} \end{bmatrix} \quad 5.5$$

where i_r the starting is reference symbol index and ω can be specified as $2\pi/N_{DFT}$ with N_{DFT} being the DFT size.

Similar to equation 4, we can write for the transmitted data symbols as follows:

$$Y = X_d T_d h + \mu_d \quad 5.6$$

$$T_d = \frac{1}{\sqrt{N_{DFT}}}\begin{bmatrix} e^{-j\omega(i_d)(0)} & e^{-j\omega(i_d)(1)} & \dots & e^{-j\omega(i_d)(L-1)} \\ e^{-j\omega(i_d+1)(0)} & e^{-j\omega(i_d+1)(1)} & \dots & e^{-j\omega(i_d+1)(L-1)} \\ \vdots & \vdots & \ddots & \vdots \\ \vdots & \vdots & \ddots & \vdots \\ e^{-j\omega(i_d+N_d-1)(0)} & e^{-j\omega(i_d+N_d-1)(1)} & \dots & e^{-j\omega(i_d+N_d-1)(L-1)} \end{bmatrix}$$

5.3) Pilot-assisted Channel Estimation

The pilot assisted channel estimation process consists of two steps; first statistical estimation of the channel at OFDM tones consisting of reference symbols is determined using statistical methods including Squares (LS) and Minimum Mean Squares (MMSE) estimates.

Different pilots assisted channel estimation schemes can be employed for the estimation of the channel effects on the transmitted signal. The response of the channel at the data subcarriers is subsequently determined by interpolation. The interpolators used for the purpose of estimation are linear, second order, cubic or

time domain interpolators derived from both the statistical and deterministic point of view [46,47,48]. Various publications can be found that deal with one or all these estimation criteria for pilot assisted channel estimation of OFDM applications from CIR or CFR prospective [49,50,51,52,53,54].

In this chapter, we attempt to give an overview of these estimation techniques with a reference to LTE down link structure described in chapter 2.

5.3.1) Least Square Estimation

Least Square based parameter estimation approach aims at determining the channel impulse response from the known transmitted reference symbols in the following way:

$$G_{LS} = \left[\frac{Y_{r(1)}}{X_{r(1)}}, \frac{Y_{r(2)}}{X_{r(2)}}, \frac{Y_{r(3)}}{X_{r(3)}}, \ldots \frac{Y_{r(N)}}{X_{r(N)}}\right] \qquad 5.7$$

where $\mathrm{G_{LS}} \epsilon \mathrm{C^{N_r}}$ is the estimated channel frequency response on the subcarriers which contains reference symbols. This response can be interpolated over full frequency range in order to obtain the channel frequency response for the subcarriers carrying data symbols. The interpolation can be performed in time domain or frequency domain.

The signal received in time domain can be expressed as follows:

$$Y_r = F^H A_r F_L h + \mu \qquad 5.8$$

The channel can be estimated using Least Squares, in time domain in the following way [45]:

$$\hat{h} = (S^H S)^{-1} S^H Y_r \qquad 5.9$$

Solving the above two equations, we get the expression for LS estimates.

$$\hat{h} \approx (F_L^H A_r^H A_r F_L)^{-1} F_L^H A_r^H F^H Y_r \qquad 5.10$$

The term $(\mathrm{F_L^H A_r^H A_r F_L})^{-1}\mathrm{F_L^H}$ in this equation is constant and can be computed offline regardless of the time varying nature of the channel. This makes LS estimator computationally simple. However an ill-conditioned problem occurs in straightway application of LS estimator due to matrix inversion. The problem can be solved in the following two ways [46].

5.3.2) Regularized LS Estimation

In this method, small constant term is added to the diagonal entries for regularizing the Eigen values of the matrix to be inverted. In this case, the channel impulse response becomes of the form,

$$\hat{h}_{reg} = (\alpha I + F_L^H A_r^H A_r F_L)^{-1} F_L^H A_r^H F^H Y_r \qquad 5.11$$

The value of α has to be selected such that the inverse matrix is least perturbed.

5.3.3) Down Sampling Method

The second solution to the ill-conditioning problem is found by considering the fact that not all portion of the spectrum is used due to LTE OFDM symbols structure. Consider the case of 5 MHz bandwidth, the number of used (modulated) subcarriers is 300. The sampling frequency in this case is 7.68 MHz so the bandwidth is 4.5 MHz in this case. Here we want to achieve occupied bandwidth close to the sampling frequency. This can be achieved by down sampling by a factor of 2/3 of the sampling frequency. Practically, the channel is not estimated over all taps but only 2 out of 3 taps are estimated to obtain a down sampling factor of 2/3 [46].

$$\hat{h} = (h_0, h_1, 0, h_3, h_4, 0 \ldots h_{L-1})^T$$

$$F_L^{DS} h^{DS} = \frac{1}{\sqrt{N_{DFT}}} \begin{bmatrix} f_{(1,1)} & f_{(1,2)} & f_{(1,4)} & \cdots & \cdots & f_{(1,L)} \\ f_{(2,1)} & f_{(2,2)} & f_{(2,4)} & \cdots & \cdots & f_{(2,L)} \\ \vdots & \vdots & \vdots & \ddots & & \vdots \\ \vdots & \vdots & \vdots & \ddots & & \vdots \\ f_{(N,1)} & f_{(N,2)} & f_{(N,4)} & \cdots & \cdots & f_{(N,L)} \end{bmatrix} \begin{bmatrix} h_0 \\ h_1 \\ h_3 \\ \vdots \\ \vdots \\ h_{L-1} \end{bmatrix}$$

By removing every third column of the matrix, we get $\mathrm{F_L^{DS}} \epsilon \mathrm{C}^{\mathrm{N_{IFFT} \times L_{DS}}}$ and complexity is reduced. Now the time domain representation of the received signal can be written as follows:

$$Y_r = F^H A F_L^{DS} h^{DS} + \mu_r \qquad 5.12$$

The LS channel response can be formulated as follows:

$$\hat{h}_{DS} = (F_L^{DS,H} A_r^H A_r F_L^{DS})^{-1} F_L^{DS,H} A_r^H Y_r \qquad 5.13$$

The channel impulse response can be transformed back into frequency domain by multiplying it by the matrix $\mathrm{F_t^{DS}}$ which is truncated version of $\mathrm{F_L^{DS}}$ with rows corresponding to the position of the data symbols.

5.3.4) Minimum Mean Square Estimation

In the above section, LS channel estimation method has been described which is computationally simple but its performance is not good. Another method to estimate the CIR is minimum mean square estimator (MMSE) which has better performance than LS but it is computationally complex. This method intends at the minimization of the mean square error between the exact and estimated CIRs. In this section we will discuss linear minimum mean square estimator (LMMSE). The CIR can be calculated using LMMSE in the following way [45]

$$\hat{h} = R_{hY_r} {R_{Y_rY_r}}^{-1} Y_r \qquad 5.14$$

Here $\mathrm{R_{Y_rY_r}}$ is the auto covariance of vector $\mathrm{Y_r}$ and $\mathrm{R_{hY_r}}$ is the cross covariance of vectors h and $\mathrm{Y_r}$.These covariance matrices for the above equation can be calculated as,

$$R_{Y_rY_r} = E\left[Y_r {Y_r}^H\right] \qquad 5.15$$

$$= E[(X_r T_r h + \mu_r)(X_r T_r h + \mu_r)^H]$$

$$= E\left[(X_r T_r h + \mu_r)({X_r}^H {T_r}^H h^H + {\mu_r}^H)\right]$$

$$= X_r T_r E[hh^H] {X_r}^H {T_r}^H + E[\mu_r {\mu_r}^H] + X_r T_r [h {\mu_r}^H] + [\mu_r h^H] {X_r}^H {T_r}^H$$

$$= X_r T_r R_{hh} {X_r}^H {T_r}^H + \sigma_\mu^2 I_{N_r} \qquad 5.16$$

$$R_{hY_r} = E\left[h {Y_r}^H\right] \qquad 5.17$$

$$= E[hh^H {X_r}^H {T_r}^H + \mu_r h^H {X_r}^H {T_r}^H]$$

$$= R_{hh} {X_r}^H {T_r}^H = {X_r}^H {T_r}^H \qquad 5.18$$

$$\hat{h} = {X_r}^H {T_r}^H (X_r T_r R_{hh} {X_r}^H {T_r}^H + \sigma_\mu^2 I_{N_r})^{-1} Y_r \qquad 5.19$$

5.4) Equalization

After estimating the channel impulse response, we now turn our attention for equalization of the received data blocks. Due to time domain convolution, the received subcarriers in OFDM data block suffer from distortion on their amplitude and shift in their phases. This is caused by multiplicative complex channel coefficients on each subcarrier. Equalization can be performed in order to combat the multiplicative effects imparted by the multipath channel on the subcarriers of

the OFDM symbols. We consider two equalization options; equalization in time domain and equalization in frequency domain.

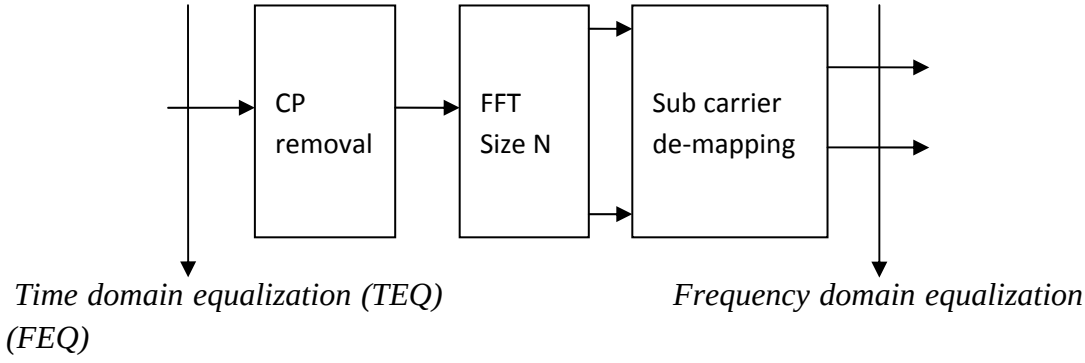

Figure 5.1: Equalizer options for LTE, in time domain and frequency domain.

Firstly, we can position the equalizer on time domain data symbols and try to make these received symbols as close as possible to the transmitted symbols as shown in figure 5.1. This is called time domain equalization (TEQ) which computationally complex method. The time domain equalization has been used for scenarios in OFDM systems where the performance of other equalizer structures is not significant as in the case of time varying propagation conditions [55, 56, 57].

The second method to design equalizer for reducing the error between transmit and receive subcarriers is frequency domain equalizer (FEQ). The frequency domain equalizer is simple and computationally less complex as compared to time domain equalizer [58]. In the case of frequency domain equalization the received signal is first transformed into frequency domain by means of N-point DFT and then equalization is performed as frequency domain filtering. In our work we have performed frequency domain linear equalization for the received data symbols.

Consider the frequency domain system model illustrated in equation 5.6 which is repeated here for convenience,

$$Y = X_d T_d h' + \mu_d' \qquad 5.20$$

Where $\mathrm{X_d}$ is a diagonal matrix containing the data symbols, $\mathrm{T_d}$ is Fourier matrix associated with the data symbols and μ_d' is the additive white Gaussian noise.

Since $\mathrm{X_d}$ is a diagonal matrix, we can write for the $\mathrm{i^{th}}$ data subcarrier as,

$$Y_d(i) = X_d(i)E_d(i) + \mu_d' \qquad 5.21$$

Here $\mathrm{E_d(i)}$ is the $\mathrm{i^{th}}$ element of$\mathrm{T_d h'}$. Finally we can write LMMSE estimate for the received data in the following form.

$$\hat{X}_d(i) = (E_d(i)^*/\|E_d(i)\|^2 + \sigma_n^2)Y_d(i) \qquad 5.22$$

5.5) Performance Comparison of Channel Estimation Schemes

We simulate LTE down link single-input single-output (SISO) system with the parameters given in the specification [3].The system bandwidth is selected 15 MHz with the numbers of subcarriers 1536 out of which 900 subcarriers are used and the remaining are zero padded. The sub frame duration is 0.5ms which leads to a frame length of 1sec. This corresponds to the sampling frequency of 23.04 MHz or sampling interval of 43.4ns. A cyclic prefix of length 127 (selected from specification which is extended CP) is inserted among data subcarriers to render the effects of multipath channel which completely removes ISI and ICI. In simulating the SISO system, only one port of an antenna is considered and this antenna port is treated as physical antenna. We consider one OFDM symbol of size 900 subcarriers and the reference symbols which are (total numbers of

reference symbols are 150) distributed among data subcarriers according to specifications [3] transmitted from the antenna during one time slot. The constellation mappings employed in our work are QPSK, 16 QAM and 64 QAM.

The channel models used in the simulation are ITU channel models [42]. These models are described in chapter 4. At the receiver end we used regularized LS and LMMSE estimation methods for the channel estimation. All channel taps are considered independent with equal energy distribution. Also frequency domain linear equalization is carried out on the received data symbols. The performance of the system is measured by measuring bit error rates and symbol error rates using ITU channel models with different modulation schemes.

The designed simulator is flexible to use. A scalable bandwidth is used, i.e., there is option for using bandwidths of 5 MHz,10 MHz, 15 MHz and 20 MHz. In addition, cyclic prefixes of different lengths specified in [3] can be easily selected in the simulation of the system. We used single port of antenna which is taken as physical antenna however changes can be easily made to include two ports antenna. A block diagram of the SISO system used in simulations is illustrated in figure 3.1 in chapter 3.

The performance of LTE transceiver is shown in terms of curves representing BER and SER against SNR values and is compared with AWGN for different channel models. Figures 5.2 and 5.4 illustrate BER versus SNR for LMMSE and LS channel estimations, respectively for different ITU channel models using QPSK modulation. Figures 5.3 and 5.5 show SER for the two estimation techniques respectively, for different channel models employing QPSK modulation scheme. From these figures, it can be seen that LMMSE channel estimation gives better performance than LS channel estimation. Figures 5.5 and 5.7 are BER and figures 5.6 and 5.8 are SER plots for ITU channel models using 16QAM modulation technique.

It is seen that by increasing the modulation order, the system performance degrades as compared to QPSK modulation. This is due to the fact that higher modulations schemes are more sensitive to channel estimation errors and delay spreads. For 16QAM, LMMSE still have superior performance as compared to LS estimation but its performance also diminishes in environments with high mobile speeds (Doppler spread) and large delay spreads. The LS estimation gives poor performance for higher modulation schemes. Some interpolation techniques can be employed to mitigate ISI effects which can enhance system performance.

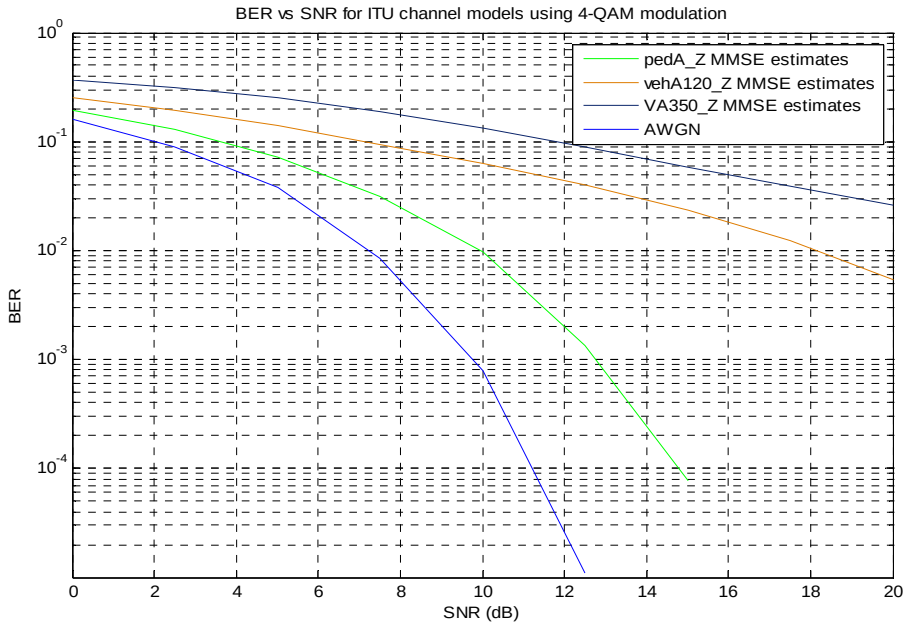

Figure 5.2: BER performance of LTE transceiver for different channels using QPSK modulation and LMMSE channel estimation

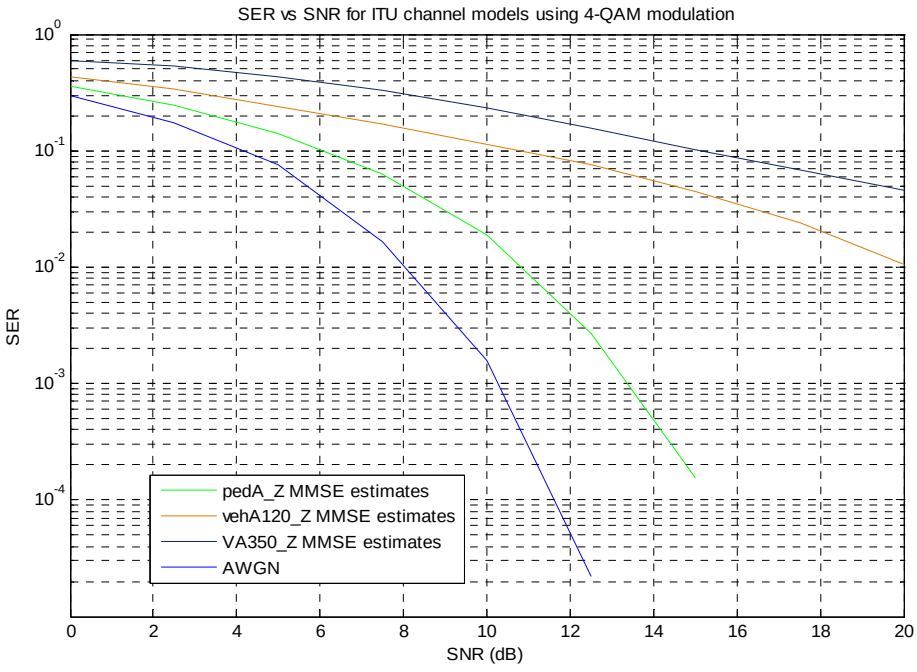

Figure 5.3: SER performance of LTE transceiver for different channel models using QPSK modulation and LMMSE channel estimation

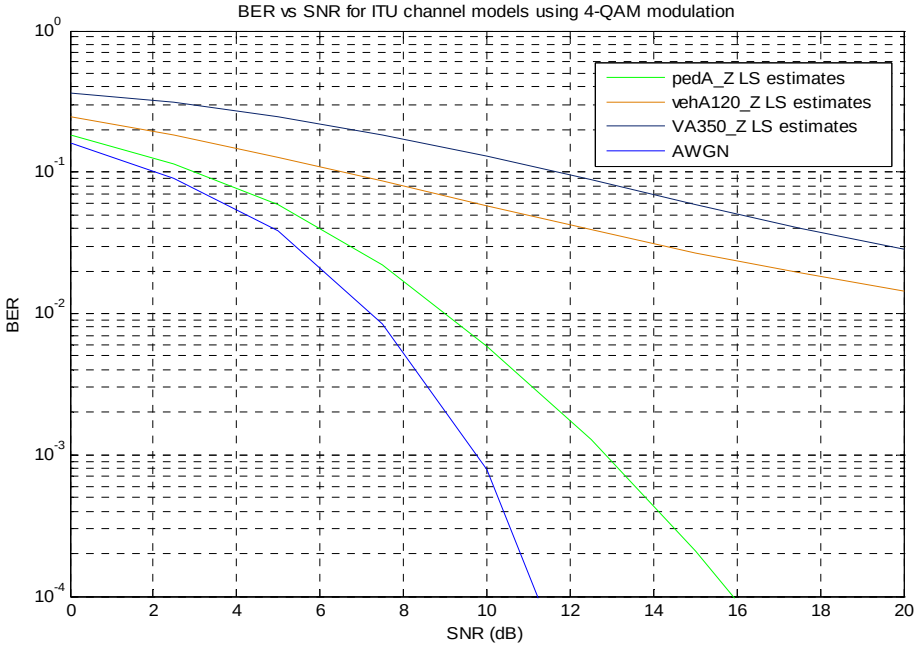

Figure 5.4: BER performance of LTE transceiver for different channel models using QPSK modulation and LS estimation

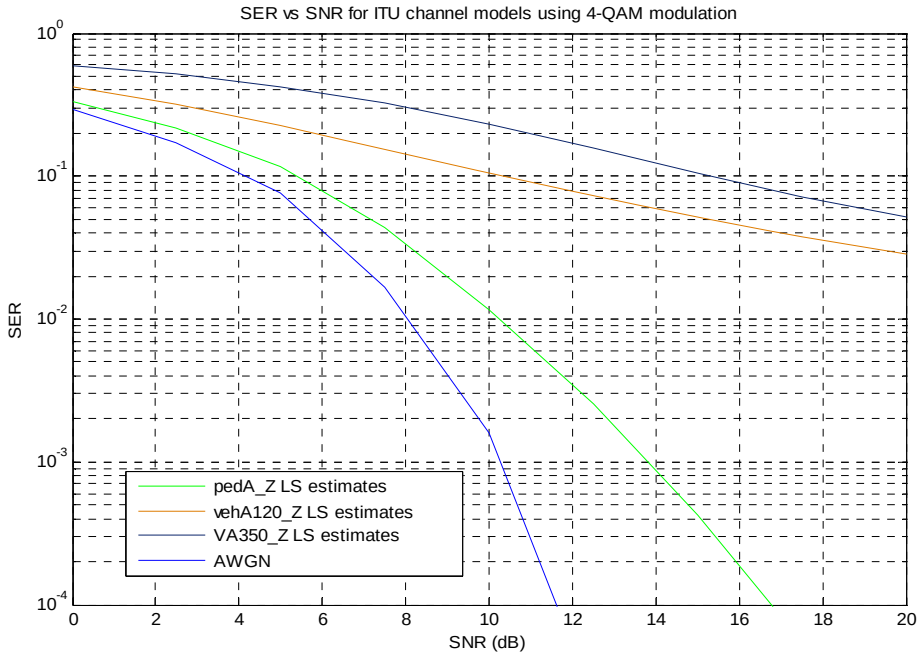

Figure 5.5: SER performance of LTE transceiver for different channel models using QPSK modulation and LS channel estimation

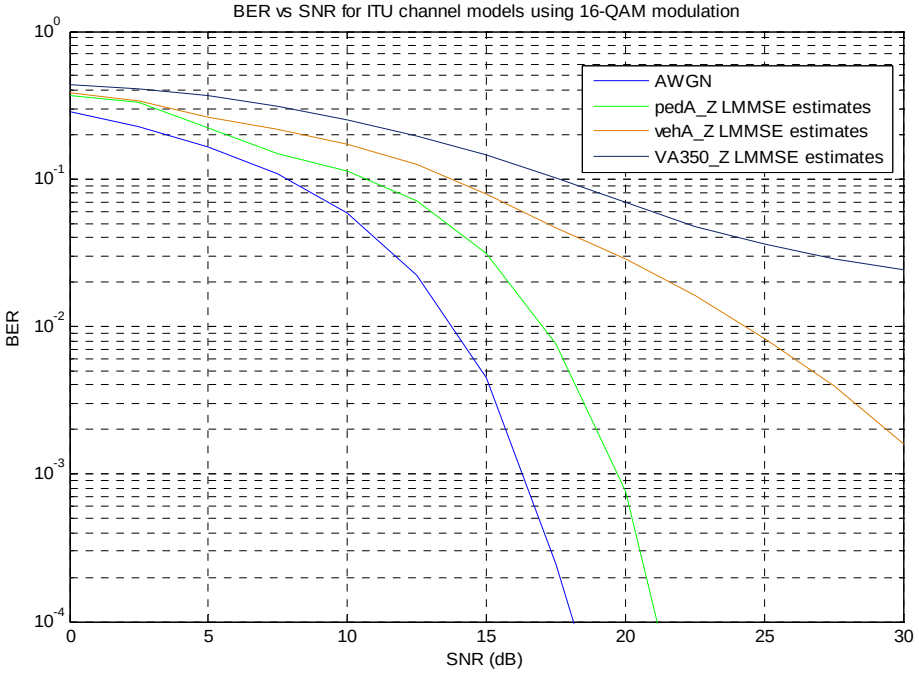

Figure 5.6: BER performance of LTE transceiver for different channel models using 16 QAM modulation and LMMSE channel estimation

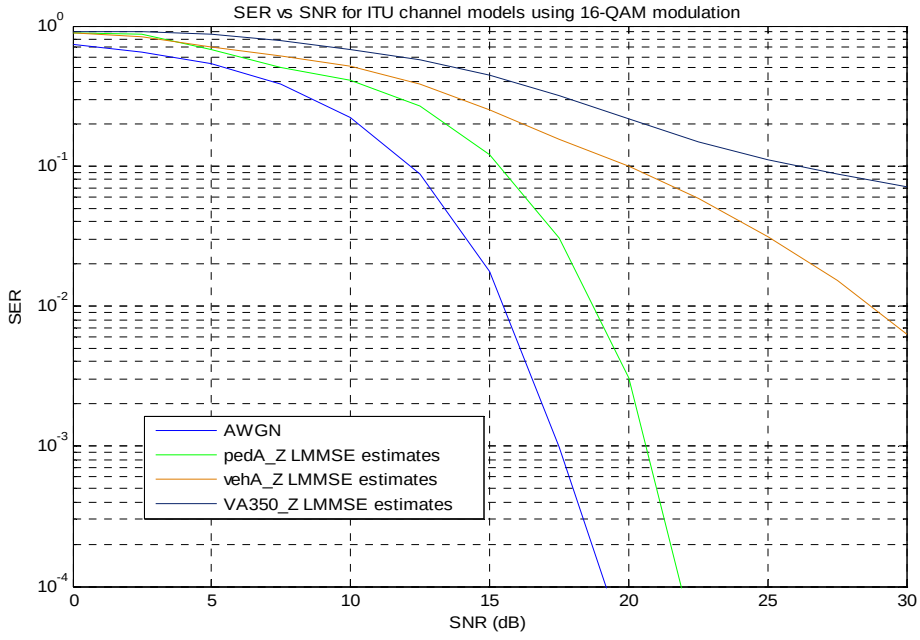

Figure 5.7: SER performance of LTE transceiver for different channel models using 16 QAM modulation and LMMSE channel estimation

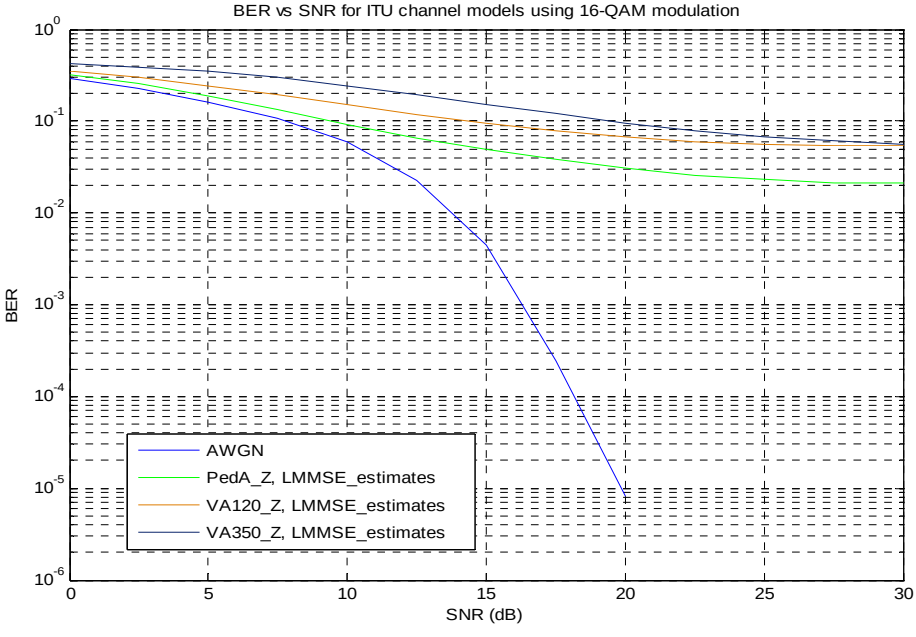

Figure 5.8: SER performance of LTE transceiver for different channel models using 16-QAM modulation and LS channel estimation

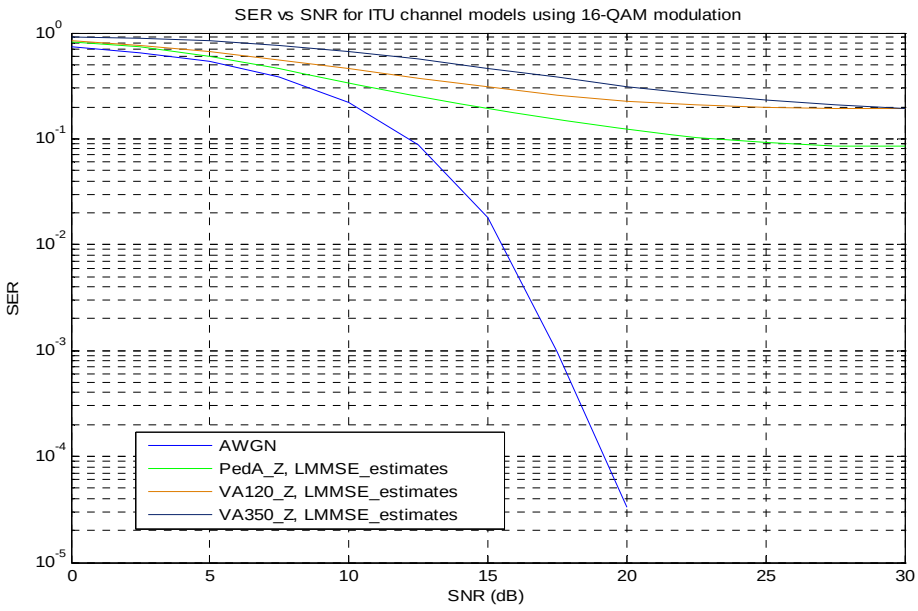

Figure 5.9: SER performance of LTE transceiver for different channel models using 16-QAM modulation and LS channel estimation

Chapter 6 Channel Estimation for Multiple Antenna Systems

6.1) Introduction

Signals following multipaths suffer from deep fades due to destructive interference and have low amplifications and high phase derivatives which often render their accurate detection difficult. Diversity techniques, discussed in chapter 2, have the most promising features in modern wireless communications to combat such phenomenon. OFDM has great capability to mitigate inter-symbol interference and channel frequency selectivity and provides high data rates in wideband wireless channels. In OFDM symbols, the subcarriers are regularly spaced with the minimum frequency separation required to retain orthogonality. Thus OFDM systems hold with them an inherent diversity in the frequency domain. By selecting the sub-carrier spacing appropriately in relation to the channel coherence bandwidth, a frequency selective channel can be converted into parallel independent frequency flat channels using OFDM. Algorithms that are appropriate for frequency flat channels can then be directly applied. In practical OFDM systems, channel coding and interleaving across the subcarriers can be used to achieve frequency diversity [59, 60].

In this work we will not deal with channel coding and interleaving to achieve frequency diversity. Wireless systems employing MIMO techniques can take the benefit from dense scattering environment to improve the spectrum efficiency. The combination of MIMO-OFDM is the most promising scheme for future generation mobile cellular systems air interface. STBC (see chapter 3) can provide full diversity for MIMO systems, but full transmission rate cannot be achieved

when number of transmitting antennas is greater than two. However, in case of LTE frequency domain version of STBC, SFBC is used [61] to exploit diversity.

In this chapter we will use MIMO-SFBC in LTE down link to evaluate channel estimation algorithms. Channel estimation techniques are discussed in chapter 5.

6.2) SFBC in LTE

In this section we will discuss SFBC in LTE down link briefly from simulation prospect. The technique is discussed in details in chapter 3. SFBC can realize full space diversity but is not guaranteed to achieve full (space and frequency) diversity [62]. OFDM symbols transmitted from two and four antennas, respectively, can be written in matrices form as follows:

Space

$$G1 = \begin{bmatrix} s_o & -s_1^* \\ s_1 & s_0^* \end{bmatrix} \downarrow \text{ Frequency} \qquad 6.1$$

Space

$$G\,2 = \begin{bmatrix} s_0 & 0 & -s_1^* & 0 \\ s_1 & 0 & s_0^* & 0 \\ 0 & s_2 & 0 & -s_3^* \\ 0 & s_3 & 0 & s_2^* \end{bmatrix} \downarrow \text{ Frequency} \qquad 6.2$$

From the matrices it can be observed that the SFBC with 4 transmit antennas is a simple superposition of SFBC with 2 transmit antennas. It is found that without using channel coding and interleaving, raw bit error rate (BER) performance of 4-antenna SFBC is similar to 2-antenna SFBC. Therefore in this work, we restrict to 2-antenna SFBC system for evolution of channel estimation techniques. The model used in simulations is shown in figure 6.1.

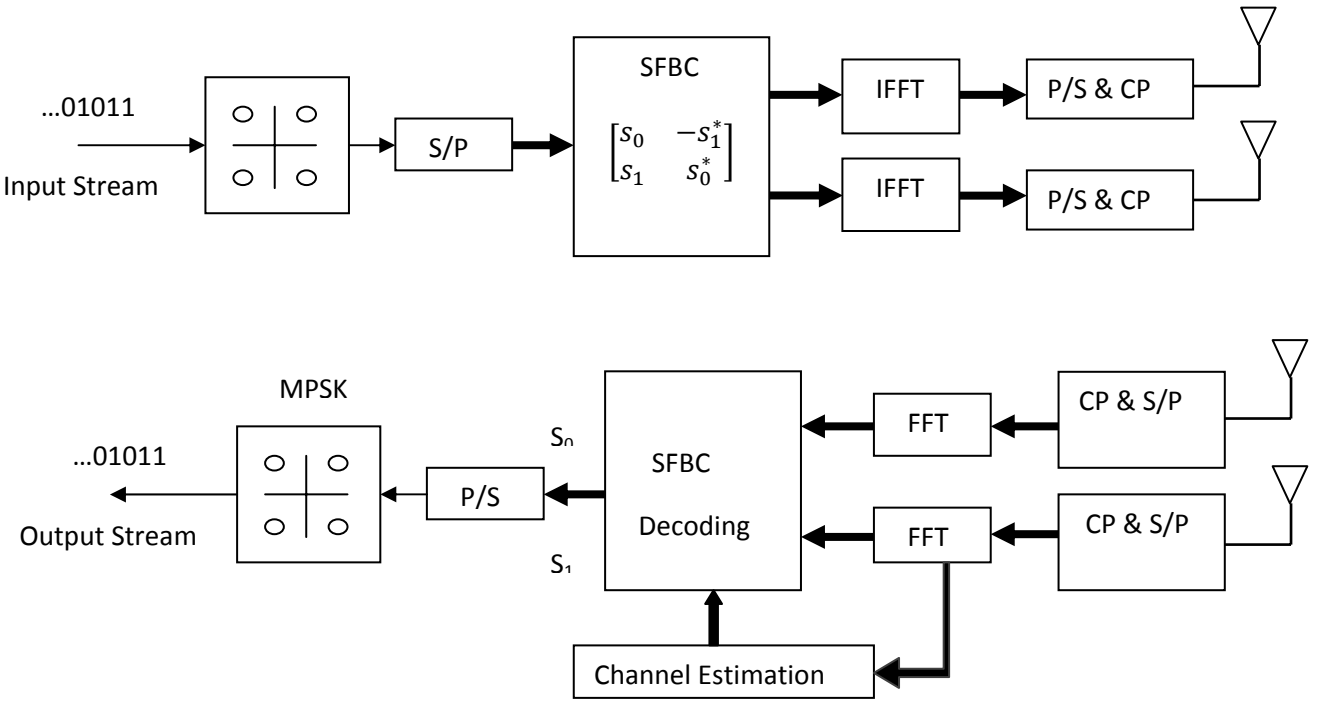

Figure 6.1: System model for simulation of 2x2 MIMO-OFDM using SFBC

The received OFDM symbols can be written as follows:

$$\begin{bmatrix} y_1 \\ y_2 \end{bmatrix} = \frac{1}{\sqrt{2}} \begin{bmatrix} h_{00} & -h_{01} \\ h_{11}^* & h_{10}^* \end{bmatrix} \begin{bmatrix} s_0 \\ s_1^* \end{bmatrix} + \begin{bmatrix} n_0 \\ n_1^* \end{bmatrix} \qquad 6.3$$

In equation 6.3 $h_{(i,j)}$ (i, $j \epsilon \{0, 1\}$) represents the channel response at the i^{th} symbol from transmit antenna j and n_0, n_1 are complex additive white Gaussian noises with identical correlation matrices of $\sigma^2 I_N$.

6.3) Channel Estimation and Decoding

The techniques used to find estimates are discussed in chapter 5 for SISO systems. In this section, we will discuss estimation techniques from multiple antennas

prospect. After receiving the signals on the respective antennas, first channel estimation is performed. The reference symbols which are allocated specific subcarriers according to [3] are extracted from the received signals to find the channel estimates. The received signals at the pilot locations can be written as follows [63]:

$$\begin{bmatrix} X & 0_{N\times N} \\ 0_{N\times N} & X \end{bmatrix}\begin{bmatrix} y_1 \\ y_2 \end{bmatrix} = \frac{1}{\sqrt{2}} S_r \begin{bmatrix} X & 0_{N\times N} \\ 0_{N\times N} & X \end{bmatrix}\begin{bmatrix} h_0 \\ h_1 \end{bmatrix} + \begin{bmatrix} n_0 \\ n_1 \end{bmatrix} \quad 6.4$$

In equation 6.4, X = diag{$x(1)$, $x(2)$...$x(N)$} represents a diagonal matrix, where $x(i) \in \{0,1\}$ for $1 \leq i \leq N$. If the i^{th} subcarrier is a reference symbol, then $x(i) = 1$ and $x(i) = 0$ otherwise. Mathematical derivations of channel estimation algorithms for MIMO case can be found in [64,65]. Let $\widehat{H}$ be the estimate of channel impulse responses at the pilot symbols:

$$\widehat{H} = H + \widetilde{H}$$

$\widetilde{H}$ is zero mean complex circular white noise vector. The desired signal after maximum likelihood decoding [66] is written as follows:

$$Z = \widehat{H}^H Y = \frac{1}{\sqrt{2}}(H^H + \widetilde{H}^H)\frac{1}{\sqrt{2}}(Hs + n) \quad 6.5$$

$$= \frac{1}{2}\begin{bmatrix} |h_{00}|^2 + |h_{11}|^2 & h_{10}^* h_{11} - h_{00}^* h_{01} \\ h_{10}h_{11}^* - h_{00}h_{01}^* & |h_{10}|^2 + |h_{01}|^2 \end{bmatrix} s + \frac{1}{2}\widetilde{H}^H H s + \frac{1}{\sqrt{2}}\left(H^H + \widetilde{H}^H\right) n \quad 6.6$$

$$= \frac{1}{2}\begin{bmatrix} (|h_{00}|^2 + |h_{11}|^2)s_0 \\ (|h_{10}|^2 + |h_{01}|^2)s_1^* \end{bmatrix} + \frac{1}{2}\begin{bmatrix} (h_{10}^* h_{11} - h_{00}^* h_{01})s_1^* \\ (h_{10}h_{11}^* - h_{00}h_{01}^*)s_0 \end{bmatrix} + \frac{1}{2}\widetilde{H}^H H s \quad 6.7$$

$$+ \frac{1}{\sqrt{2}}\left(H^H + \widetilde{H}^H\right) n \quad 6.8$$

The first term in equation 6.7 gives the desired data symbols after decoding while second term represents self-interference. Equation 6.8 denotes additive noises.

6.4) Numerical Results and Performance analysis

We simulated a SFBC-OFDM system with 2x1 and 2x2 multiple antenna systems. We considered the following simplifications to ease our simulation for LTE down link.

- We used bandwidth 15 MHz where the number of used subcarriers is $N_{sc} = 1536$ and the subcarriers spacing $\Delta f = 15\ \mathrm{kHz}$. The sampling time is 43.40 ns. Within the simulator, there is option of selecting bandwidths of 5MHz, 10 MHz and 20 MHz
- In the simulator, two types of CP lengths can be selected: short cyclic prefix and extended cyclic prefix according to [3].
- QPSK, 16QAM and 64 QAM modulation schemes can be used in simulations.
- Channel models, pedestrian-A (3 km/h), vehicular-A (120 km/h) and vehicular-A (350 km/h) based on ITU recommendations [42] for LTE are used in simulations.
- We used one port of an antenna and it is considered as physical antenna.
- Reference symbols are slotted-in according to [3] and channel estimation is employed using MMSE estimates.

The system is simulated for 2x2 and 2x1 systems, and the results from chapter 5 are used here for comparison purposes. The system is simulated using QPSK modulation and LMMSE estimation is used for channel estimates. The delay spreads always have impact on BER and SER: delay spreads introduce self interferences which result in smaller SINR. For ITU Pedestrian-A model, the delay

spread is 11µs [42] and the length of CP is 16.67µs (table 2.2). Thus, because of small delay spread, the influence of ISI is eliminated and a good performance in terms of BER and SER is attained in all three cases as shown in figure 6.2 and figure 6.3, respectively. It is obvious from figures that diversity gain is also achieved because of multiple antenna arrays. From figures 6.4 and 6.5 for ITU Pedestrian-B model and from figures 6.6 and 6.7 for ITU vehicular-A model, it is seen that the performance is not good as for ITU pedestrian-A model. This is due to reason that delay spreads for these channel models are large as compared to the length of cyclic prefixes. Thus, a significant ISI occurs for these channel models. In addition, the presence of large Doppler spreads causes imperfect channel estimates and the system performance further degrades. The use of multiple antenna arrays provides additional diversity gain.

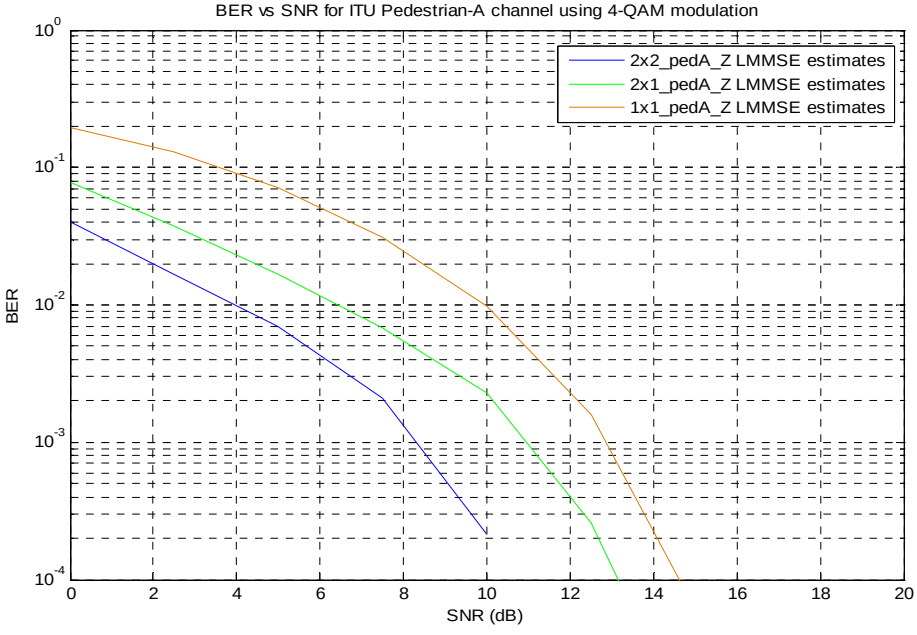

Figure 6.2: BER performance of LTE transceiver with multiple antennas for ITU Pedestrian-A channel model using QPSK modulation and LMMSE channel estimation

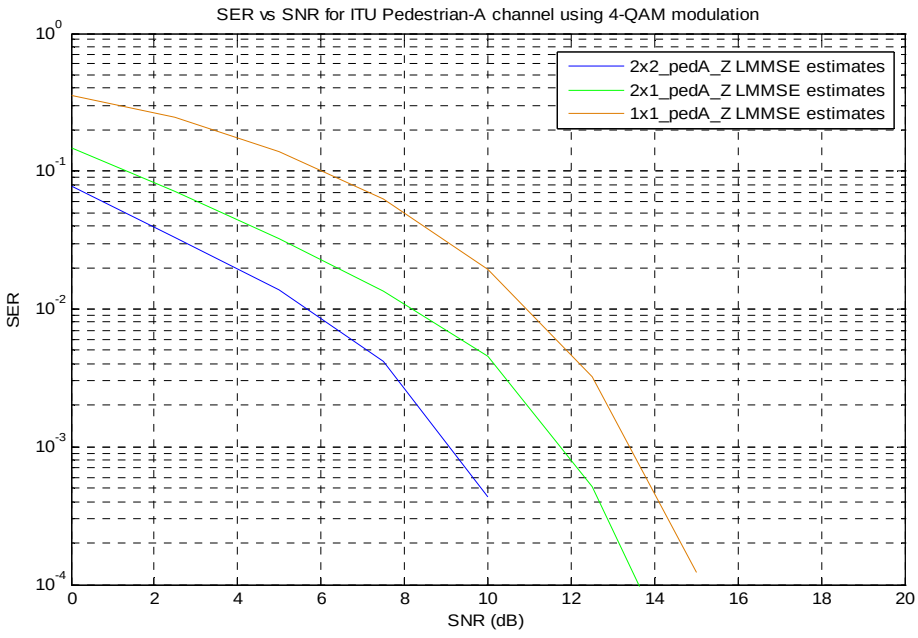

Figure 6.3: SER performance of LTE transceiver with multiple antennas for ITU Pedestrian-A channel model using QPSK modulation and LMMSE channel estimation

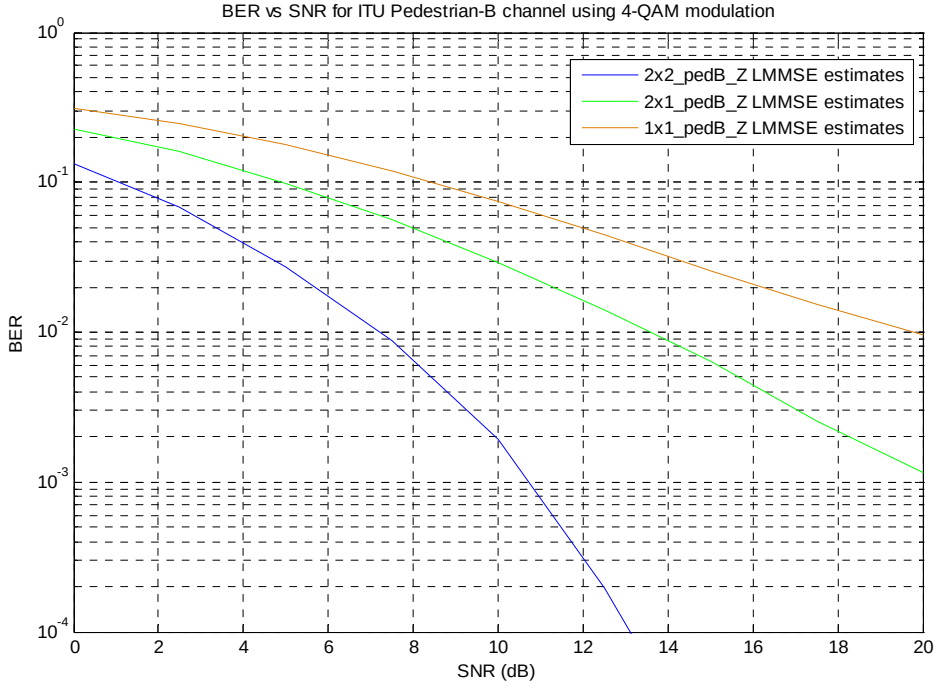

Figure 6.4: BER performance of LTE transceiver with multiple antennas for ITU Pedestrian-A channel model using QPSK modulation and LMMSE channel estimation

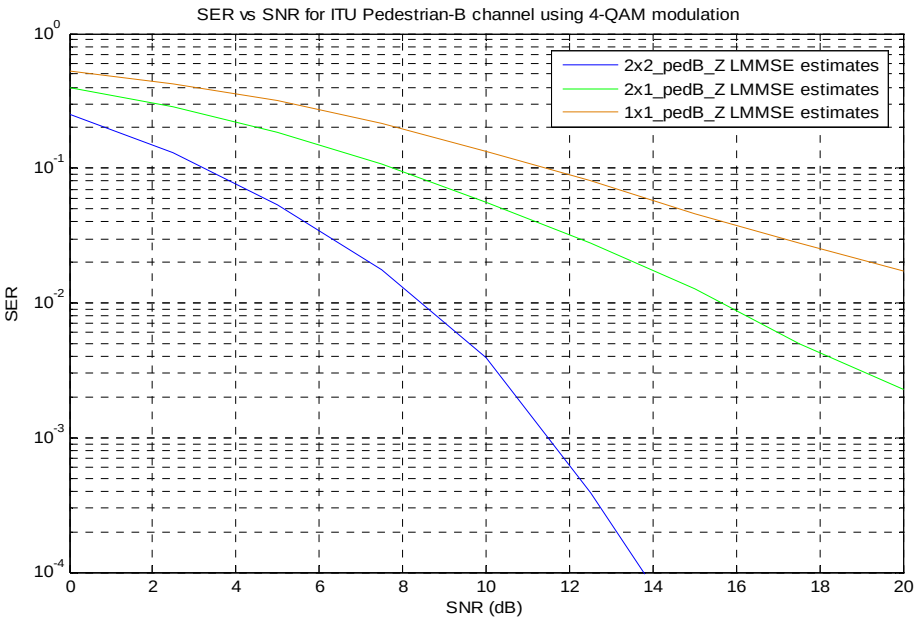

Figure 6.5: SER performance of LTE transceiver with multiple antennas for ITU Pedestrian-A channel model using QPSK modulation and LMMSE channel estimation

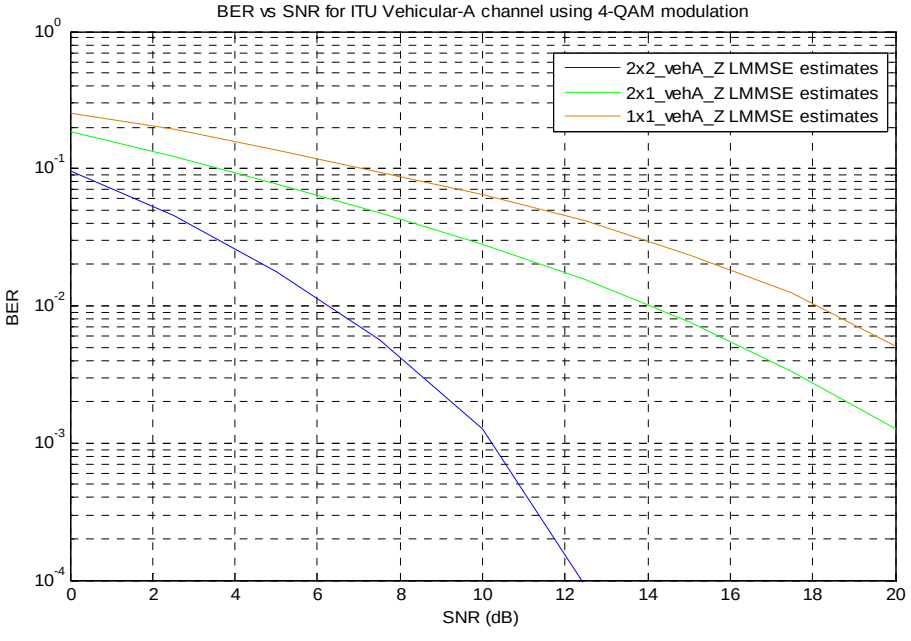

Figure 6.6: BER performance of LTE transceiver with multiple antennas for ITU Vehicular-A channel model using 4-QAM modulation and LMMSE channel estimation

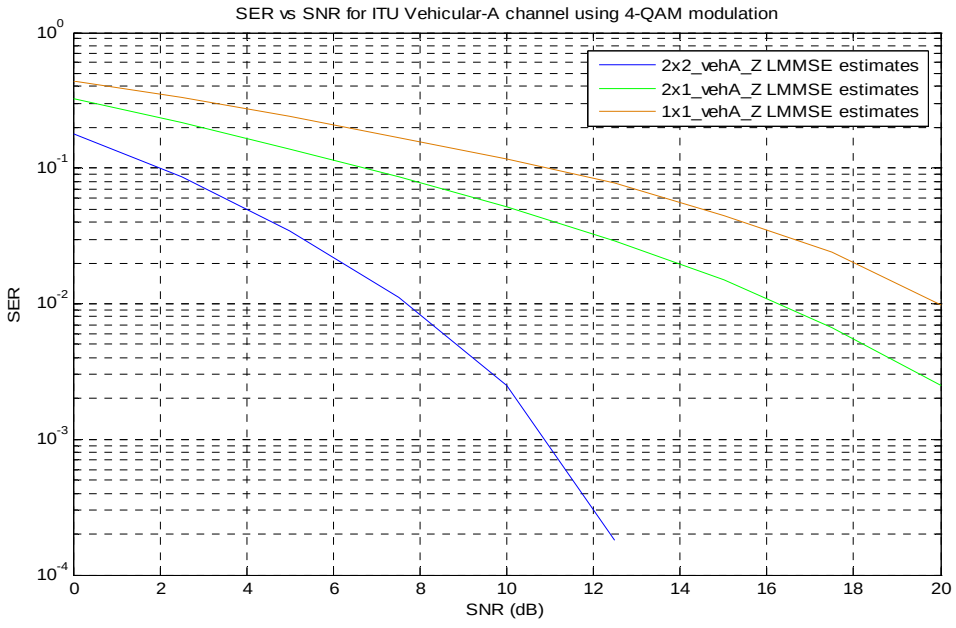

Figure 6.7: SER performance of LTE transceiver with multiple antennas for ITU Vehicular-A channel model using 4-QAM modulation and LMMSE channel estimation

Chapter 7 Conclusions

The purpose of this work is to evaluate the channel estimation schemes for LTE downlink based on 3GPP LTE downlink specifications [2]. We have focused on the task of channel estimation and equalization for OFDM based LTE downlink. The results for both, SISO and MIMO-OFDM have been presented. The work can be summarized in the following steps:

- Study of Physical layer of LTE downlink based on 3GPP specifications which includes LTE downlink frame structure in time domain and frequency domain, reference symbols structure and multiple antenna techniques for LTE.
- A link level system model has been presented in chapter 3 which employs MIMO-OFDM for LTE downlink. The model is valid for bandwidths of 5, 10, 15 and 20 MHz.
- As fading is one of the limiting factors in wireless communications, in chapter 4 details about standard channel models based on ITU recommendations have been described.
- Different channel estimation schemes for channel models discussed in chapter 4 have been described in chapter 5 for SISO system and in chapter 6 for multiple antenna systems.

The results have been presented by means of simulations. The performance is measured in terms of BER and SER and the obtained results are compared with theoretical values. The LS estimator is simple and suitable for high SNR values; however its performance degrades with higher constellation mappings for high mobile speeds. On the other hand, LMMSE estimator is computationally complex

and requires a priori knowledge of noise variance but its performance is superior to LS estimates for higher modulation schemes and large delay spreads.

References

[1] 3GPP, TR 25.913 V2.0.0, "Requirements for Evolved UTRA and Evolved UTRAN," Release 7, 2005

[2] 3GPP, Release 8 V0.0.3, "Overview of 3GPP Release 8: Summery of all Release 8 Features," November 2008

[3] 3GPP, TR 36.211 V8.7.0, "Physical Channels and Modulation," Release 8, May 2009

[4] Borko Furht and Syed A. Ahson, Long Term Evolution: 3GPP LTE radio and cellular technology, published by Taylor & Francis Group, LLC 2009

[5] Juan J. Sanchez, D. Morales-Jimenez, G. Gomez and J. T. Enbrambasaguas, "Physical Layer Performance of Long Term Evolution Cellular Technology," 16th Mobile IST and Wireless Comm. Summit, Budapest, 1-5 July 2007

[6] T. Haustein, J. Eichinger, W. Zirwas, E. Schulz, A. Forck, H. Gaebler,V. Jungnickel, S. Wahls, C. Juchems, F. Luhn, and R. Zavrtak, "MIMO-OFDM for a Cellular Deployment - Concepts, Real-Time Implementation and Measurements towards 3GPP-LTE," in Proceedings of the 15th European Signal Processing Conference (EUSIPCO 2007), Poznan, Poland, September 2007

[7] 3GPP TS 36.201 V8.3.0, "LTE Physical Layer - General Description," Release 8, April 2009

[8] D. Kliazovich1, F. Granelli, S. Redana and N. Riato, "Cross-Layer Error Control Optimization in 3G LTE," IEEE Global Telecommunication Conference, Trento, 2007

[9] Stefania Sesia, Matthew Baker, and Issam Toufik, LTE–the UMTS Long Term Evolution: From Theory to Practice, John Wiley & Sons Ltd 2009

[10] Erik Dahlman, Stefan Parkvall, Johan Sköld and Per Beming, 3G Evolution: HSPA and LTE for Mobile Broadband, Elsevier Ltd 2007

[11] 3GPP, TR 25.814 V7.1.0, "Physical Layer Aspects for Evolved Universal Terrestrial Radio Access (UTRA)," Release 7, September 2006

[12] A. A. Salwa Ali, S Thiagarajah, “A Review on MIMO Antennas Employing Diversity Techniques,” Proceedings of the International Conference on Electrical Engineering and Informatics Institute Technology Bandung, Indonesia June 17-19, 2007

[13] 3GPP, TR 25.913 V 8.0.0, “Requirements for Evolved UTRA (E-UTRA) and Evolved UTRAN (E-UTRAN),” Release 8, December 2008

[14] Lizhong Zheng, Member, IEEE, and David N. C. Tse, Member, IEEE, “Diversity and Multiplexing: A Fundamental Tradeoff in Multiple-Antenna Channels,” IEEE Transactions on Information Theory, Vol. 49, No. 5, MAY 2003

[15] David Tse and Pramod Viswanath, Fundamentals of Wireless Communication, Cambridge University Press 2005

[16] Claude Oestges and B. Clercks, MIMO Wireless Communications: From Real-World Propagation to Space-Time Code Design, Elsevier, 2007

[17] Volker Kuhn, Wireless Communications over MIMO Channels, John Wiley & Sons Ltd, 2006

[18] Agilent Technologies, MIMO Channel Modelling and Emulation Test Challenges, USA, October 7, 2008

[19] Mohinder Jankiraman, Space-Time Codes and MIMO Systems, published by Artech House Boston , London, 2004

[20] S.M. Alamouti, ‘‘A Simple Transmit Diversity Technique for Wireless Comm.,’’ IEEE Journal Select. Areas Communications, Vol. 16, No. 8, October 1998, pp. 1451–1458

[21] A. Hottinen, O. Tiekkonen, R. Whichman, Multi-antenna Transceiver Techniques and for 3G and Beyond, John Wiley & Sons 2004

[22] A. Huebner, F. Schuehlein, M. Bossert, E. Costa and H. Haas, “A Simple Space-Frequency Coding Scheme with Cyclic Delay Diversity for OFDM,” 5th European Personal Communications Conference, 2003

[23] M. I. Rahman, N. Marchetti, S. S. Das, Frank H.P. Fitzek and Ramjee Prasad, “Combining Orthogonal Space-Frequency Block Coding and Spatial Multiplexing in MIMO-OFDM System,” Center for TeleInFrastruktur (CTiF), Aalborg University, Denmark

[24] G. J. Foschini, and M. J. Gans, ‘‘On Limits of Wireless Communications in a Fading Environment When Using Multiple Antennas,’’ Wireless Personal Communications, Vol. 6, 1998, pp.311–335

[25] D. Morales-Jimenez, J. F. Paris and J. T. Entrambasaguas, “Performance tradeoffs among low-complexity detection,” International journal of communication systems Int. J.Commun. Syst. 2009; **22**:885–897

[26] ARIB, STD-T63-25.213 V7.6.0, “Spreading and modulation (FDD),” Release 7, 2008-09. www.3gpp.org

[27] 3GPP, TR 25.814 V7.1.0,"Physical layer aspects for evolved Universal Terrestrial Radio Access," UTRA, Release 7, 2006

[28] S. B. Weinstein and P. M. Ebert, “Data Transmission by Frequency Division Multiplexing 634, Using Discrete Fourier Transform,” IEEE Transactions on Communications, vol. 19, no. 5, pp. 628–October 1971

[29] T. Rappaport, Wireless Communications, Principles and Practice, Prentice-Hall, Englewood Cliffs, NJ, USA, 1996

[30] Mohamed Ibnkahla, Ed, Signal Processing for Mobile Communications, CRC Press, New York Washington, D.C., 2005

[31] Tero Ojanpera and Ramjee Prasad, WCDMA: Towards IP Mobility and Mobile Internet, Artech House Publishers, Boston, London, 2001

[32] B.H. Fleury. An Uncertainty Relation for WSS Processes and Its Application to WSSUS Systems, IEEE Transactions on Communications, 44(12):1632–1634, Dec. 1996

[33] James K. Cavers, Mobile Channel Characteristics, Kluwer Academic Publishers, New York, Boston, Dordrecht, London, Moscow, 2002

[34] J. Meinilä, T. Jämsä, P. Kyösti, D. Laselva, H. El-Sallabi, J. Salo, C. Schneider, D. Baum, ‘IST-2003- 507581 WINNER: Determination of Propagation Scenarios’, D5.2 v1.0, 2004

[35] Harri Holma and Antti Toskala, Ed, LTE for UMTS: OFDMA and SC-FDMA Base Band Radio Access, John Wiley & ISBN 9780470994016 (H/B) John Wiley & Sons Ltd, 2009

[36] A. F. Molisch, H. Asplund, R. Heddergott, M. Steinbauer, and T.Zwick, “The COST 259 vol.5, no. directional- channel model A-I: overview and

methodology," IEEE Transactions on Wireless Communications, 12, pp. 3421-3433, 2006

[37] L. M. Correia, Ed., Wireless Flexible Personalized Communications (COST 259 Final Report), John Wiley & Sons, Chichester, UK, 2001

[38] D. Sirkova, "Overview of COST 273 Part I: propagation modelling and channel characterization", Sofia, Bulgaria 29 June – 1 July 2006 http://www.lx.it.pt/cost273

[39] Nelson Costa, Student Member, IEEE, and Simon Haykin, Life Fellow, IEEE, "A Novel Wideband MIMO Channel Model and Experimental Validation", IEEE Transactions on Antennas and Propagation, VOL. 56, NO 2, FEBRUARY 2008

[40] D. S. Baum, J. Salo, G. Del Galdo, M. Milojevic, P. Kyösti and J. Hansen, "An Interim Channel Model for Beyond-3G Systems," in Proc. IEEE Vehicular Technology Conference, Stockholm, Sweden, May 2005

[41] P. Almers, E. Bonek, A. Burr, N. Czink, M. Debbah, V. Degli-Esposti, H. Hofstetter, P. Kyosti, D. Laurenson, G. Matz, A.F. Molisch, C. Oestges, and H. Ozcelik, "Survey of channel and Radio propagation models for wireless MIMO on systems," EURASIP Journal on Wireless Communications and Networking (special issue space-time channel modelling for wireless communications), 2007

[42] ITU-R M.1225 International Telecommunication Union, 'Guidelines for evaluation of radio transmission technologies for IMT-2000', 1997

[43] Ericsson, Nokia, Motorola, and Rohde & Schwarz, 'R4-070572: Proposal for LTE Channel Models', www. gpp.org, 3GPP TSG RAN WG4, meeting 43, Kobe, Japan, May 2007

[44] Mohamed Ibnkahla, Signal Processing for Mobile Communications, Hand book, CRC Press 2005

[45] Jan-Jaap van Beek, Ove Edfors, Magnus Sandell, Sarah Kate Wilson and Per Ola Börjesson, "On Channel Estimation in OFDM Systems," In proceedings of Vehicular Technology Conference (VTC'95), vol. 2, pp. 815-819, Chicago, USA, September 1995

[46] Andrea Ancora, Calogero Bona and Dirk T.M. Slock, "Down-Sampled Impulse Response Least-Square Channel Estimation for LTE OFDMA," 32nd IEEE International Conference on Acoustics, Speech, and Signal Processing Honolulu, USA, April 2007

[47] M. Morelli and U. Mengali, “A Comparison of Pilot-aided Channel Estimation Methods for OFDM Systems,” IEEE Transactions on Signal Processing, vol. 49, pp.3065–3073, December 2001

[48] P. Hoher, S. Kaiser and P. Robertson, “Pilot-Symbol-aided Channel Estimation in Time and Frequency,” in Proc. Communication Theory Mini-Conference (CTMC) within IEEE Global Telecommunication Conference (Globecom 1997) (Phoenix, USA), July 1997

[49] Z. Cheng and D. Dahlhaus, “Time versus Frequency Domain Channel Estimation for OFDM Systems with Antenna Arrays,” 6th International Conference on Signal Processing, Switzerland, Vol. 2, pp. 1340-1343, August 2002

[50] S. Coleri, A. Puri, and A. Bahai, “Channel Estimation Techniques based on Pilots arrangement in OFDM Systems,” IEEE Transactions on Broadcasting, Sept. 2002

[51] P. Y. Tasi and T. D. Chiuch, “Frequency Domain Interpolation Based Channel Estimation in Pilot-aided OFDM Systems,” IEEE 59th Vehicular Technology Conference, Milan, Italy, vol. 1, pp. 420-424, May 2004

[52] S. Yushi and Ed Martinez, “Channel Estimation in OFDM Systems,” Freescale Semiconductor, Rev. 0, Jan 2006

[53] S.Schiffermuller and V. Jungnickel, “Practical Channel Interpolation for OFDMA,” IEEE Global Telecommunication Conference, Berlin, 2006

[54] B. Le Saux, M. Herald and R. Legouable, Multi-Carrier Spread Spectrum 2007, Chapter: Robust Time Domain Channel Estimation for MIMO-OFDMA Downlink, SpringerLink, 2007

[55] R. K. Martin, K. Vanbleu, G. Ysebaert, M. Ding, B. Evans, M. Milosevic, M. Moonen, and C. R. Johnson Jr., “Unification and Evaluation of Equalization Structures and Design Algorithm for Discrete Multitone Modulation Systems,” IEEE Transactions on Signal Processing, June 2005

[56] H. Z. Jafarian, H. Khoshbin, and S. Pasupathy, “Time Domain Equalizer for OFDM Systems Based on SINR Maximization,” IEEE Transactions on Communications, vol.53, pp. 924-929, June 2005

[57] B. Sheng, Y. Zhou and X. You, “An Equalization Technique for OFDM Systems in Fast-Fading Multipath Channels at Low SNR,” IEICE Transactions on Communications, 2006

[58] D. Falconer, “Frequency Domain Equalization for Single-carrier Broadband Wireless Systems,” IEEE Communications Magazine, Vol. 40, No. 4, April 2002, Pp.58–66

[59] C. You and S. Choi, “Frequency Interleaved Multicarrier Systems with Two Kings of Spreading Codes,” IEICE Transactions on Communications, E91-B(7):2214-2223, 2008

[60] A. Batra, J. Balakrishnan, A. Dabak, R. Gharpurey, P. Fontaine, J. J. Ho, S. Lee, M. F. March and H. Yamaguchi, TI Physical Layer Proposal: Time-Frequency Interleaved OFDM, IEEE P802.15 Working Group for Wireless Personal Area Networks (WPANs), May 2003

[61] M. J. Dehghani, R. Aravind, S. Jam and K. M. M. Prabhu, “Space-Frequency Block Coding in OFDM Systems,” IEEE Region 10 Conference, vol. 1, pp. 543-546, 2004

[62] W. Su, Z. Safar, and K. J. R. Liu, “Full Rate Full Diversity Space-Frequency Codes with Optimum Coding Advantage," IEEE Transactions on Information Theory, vol. 51, no.1, pp. 229-249, Jan 2005

[63] A. Panah, B. Makouei and R. Vaughan, “Non-Uniform Pilot Symbol Allocation for Closed-loop OFDM,” IEEE Transactions on Wireless Communications, 2007

[64] Y. Li and G. Stuber, Orthogonal Frequency Division Multiplexing for Wireless Communications, Springer, ISBN 978-0387-29095-9, 2006

[65] Y. G. Li, N. Seshadri, and S. Ariyavisitakul, "Channel estimation for transmitter diversity in OFDM systems with mobile wireless channels," *IEEE* J. Selected Areas Commun., vol. 17, pp. 461-471, March 1999

[66] H. Jafarkhani, Space-Time Coding: Theory and Practice. New York, NY: Cambridge University Press, 2005